Tris(trimethylsilyl)silanides of the Heavier Alkali Metals—A Structural Study

Karl W. Klinkhammer*

Dedicated to Professor Paul von Ragué Schleyer on the occasion of his 68th birthday

Abstract: Transmetalation reactions between bis(hypersilyl)zinc $Zn[Si(SiMe_3)_3]_2$ and alkali metals have already been established as a facile route to powders of the solvent-free potassium, rubidium, and cesium derivatives of tris(trimethylsilyl)-silane (hypersilane, $(Me_3Si)_3SiH$).[1, 2] By the use of boiling *n*-heptane as the solvent, the hitherto unknown $NaSi(SiMe_3)_3$ (**1**) along with the previously synthesized $KSi(SiMe_3)_3$ (**2**) have now been obtained as colorless crystalline materials. Information from NMR and Raman spectra in conjunction with the acute Si-Si-Si angles found in their molecular structures indicate mainly ionic bonding. This was verified by population analyses of suitable model systems. Both hypersilanides[2] consist of cyclic dimers $[MSi(SiMe_3)_3]_2$ (**1a**, M = Na; **2a**, M = K) with almost planar M_2Si_2 rings (Na–Si = 299 pm (av); K–Si = 339 pm (av)), which are linked up into coordination polymers. In a similar manner to the related rubidium and cesium derivatives, a pentane suspension of the potassium compound afforded a yellow solution on addition of benzene, from which the crystalline, bright yellow tris(benzene) solvate **2**·(benzene)$_3$ (**2b**) was isolated. Complex **2b** consists of monomers containing short K–Si bonds (332–334 pm) and three η^6-bonded benzene molecules. No solvate of **1** was obtained under these conditions. However, on crystallization from pure benzene, crystals of (**1**)$_2$·benzene (**1b**) were isolated (Na–Si = 302 pm (av)). Benzene was found to be intercalated between rods of coordination polymers of (**1**)$_2$. In addition, the influence of π or σ donors on the molecular and crystal structures of hypersilylrubidium (**3**) and cesium (**4**) was investigated. The structures of the tetrahydrofuran solvate (**4**)$_2$·THF (**4c**), the biphenylene/pentane complex (**4**)$_2$·biphen·(pentane)$_{0.5}$ (**4b**) along with the known toluene solvates (**3**)$_2$·toluene (**3a**) and (**4**)$_2$·(toluene)$_3$ (**4a**)[1a] are compared. Finally, an example is presented of how the alkali metal hypersilanides could be utilized in preparing extremely bulky stannanide anions.

Keywords
ab initio calculations · alkali metals · Si ligands · silicon · structure elucidation

Introduction

Alkali metal silanides M^I-SiR_3 (R = alkyl, aryl, triorganylsilyl etc.), especially the lithium derivatives (M^I = Li), have been frequently used in the preparation of silyl derivatives of other elements.[3] They are usually introduced as the ether solvates, because of their facile syntheses and solubility in organic solvents. However, their applicability is limited by side reactions, such as deprotonation and cleavage of the coordinating donor ligand as well as the by formation of ate complexes or other undesirable solvated products.[4] To my knowledge, solvent-free derivatives of lithium and solvated or unsolvated analogues of the heavier alkali metals have been employed very rarely so far, although some compounds were first synthesized more than 40 years ago by Benkeser, Gilman, Wiberg, and others.[5] The main reason for this seems to be their extreme reactivity. Once formed, most compounds of this type readily react with all the organic solvents in which they are soluble. Potassium triethylsilanide, for instance, deprotonates even weak acids such as benzene or toluene to yield potassium hydride and triethylphenylsilane or benzyltriethylsilane, respectively.[4a] With the exception of a few organyl-substituted lithium silanides[6] and the parent compounds $MSiH_3$ (M = K, Rb, Cs)—the latter crystallize in typical salt-type lattices[7]—no structural data are available for alkali metal silanides in which the metal is *not* coordinated by donor solvent molecules.[8]

A few years ago, we were able to demonstrate that hypersilanides of potassium, rubidium, and cesium are readily prepared as solvent-free powders by transmetalation reactions between the corresponding mercury, cadmium, or zinc silyl and the appropriate alkali metal in *n*-pentane at room temperature (Scheme 1).[1a] One drawback of this method is the long reaction time in the case of potassium (typically several days) and the failure to produce the sodium derivative, even after a reaction period of two weeks. Nevertheless, the solvent-free silanides obtained so far do not deprotonate aromatic hydrocarbons, such as benzene or toluene, nor do they cleave ethers under ambient conditions. This may be due to extensive sterical shielding of the nucleophilic center in conjunction with an intramolecular stabilization of the alkali metal complexes through $M\cdots CH_3$ interactions—as indicated by the crystal structures of

[*] K. W. Klinkhammer
Institut für Anorganische Chemie der Universität Stuttgart
Pfaffenwaldring 55, D-70569 Stuttgart (Germany)
Fax: Int. code +(711)685-4241
e-mail: kw@anorg55.chemie.uni-stuttgart.de

0947-6539/97/0309-1418 $ 17.50+.50/0

Scheme 1. Transmetalation reaction for the preparation of M^I hypersilanides (M^I = Li, Na, K, Rb, Cs; M^{II} = Zn, Cd, Hg).

the solvent-free compounds and several solvates containing aromatic hydrocarbons and ethers, such as **3b**, **4a**,[1a] **4b**, and **4c**. Nevertheless, their reactivity towards electrophiles remains high, so that temperature-sensitive hypersilyl derivatives of thallium(II),[9a] tin(II), and lead(II)[9b] can be prepared by reaction of the bis(trimethylsilyl)amides of thallium(I), tin(II), and lead(II), respectively, with $MSi(SiMe_3)_3$ at $-60\,^{\circ}C$. Presumably, analogous germanium(II) and silicon(II) species are formed initially, but they undergo rapid rearrangement to hexakis(trimethylsilyl)disilagermirane and hexakis(trimethylsilyl)trisilirane (Scheme 2).[10]

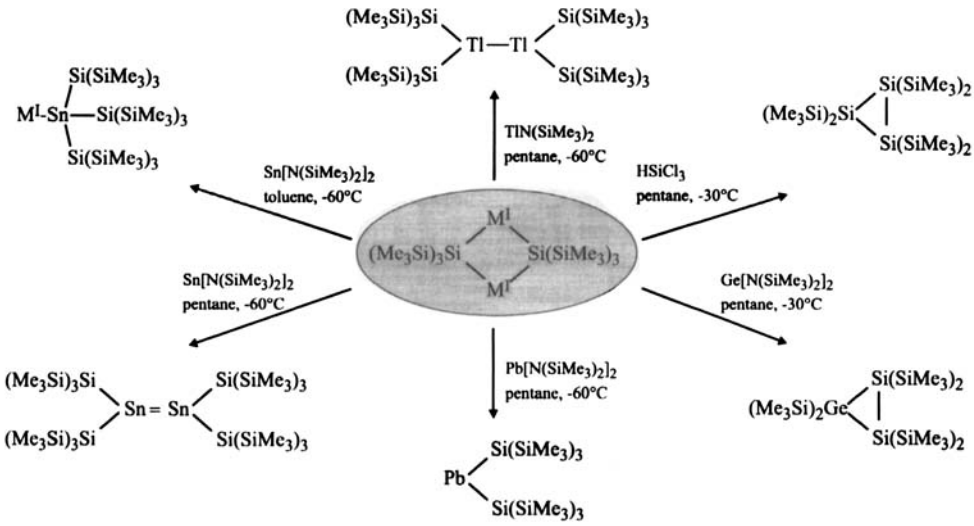

Scheme 2. Reactions of the metal hypersilanides.

By using molten alkali metal in boiling *n*-heptane, the transmetalation reaction has now been extended to the much cheaper sodium. The hitherto unknown derivative **1** could be prepared, and the synthesis of the potassium derivative **2** has

$NaSi(SiMe_3)_3$ **1**

$KSi(SiMe_3)_3$ **2**

been optimized. Both compounds can now be obtained directly as colorless crystalline materials without the need for time-consuming purification processes. The hypersilyl derivatives of the heavier alkali metals can now be investigated more thoroughly by X-ray crystallography. There are only a few molecular compounds known to date in which the heavier alkali metal atoms are not bonded to electronegative atoms such as O, N, S.

Results and Discussion

Moderate to high yields of crystalline **1** and **2** were obtained by vigorously stirring bis(hypersilyl)zinc, -cadmium, or -mercury with the appropriate molten alkali metal in boiling *n*-heptane for one day. Yields were improved by using a threefold excess of alkali metal. Crystallization from the hot-filtered mother liquors gave solvent-free, colorless crystalline products, which are highly pyrophoric. The solubility of alkali metal hypersilanides in aliphatic hydrocarbons markedly decreases with increasing atomic mass. Thus, while hypersilylsodium (**1**) dissolves readily at room temperature, the potassium derivative **2** is only sparingly soluble, and the derivatives of the higher congeners, synthesized by a similar route,[1a] do not dissolve at all.

The NMR shifts of all alkali metal derivatives recorded in benzene solutions are almost identical (Table 1). Common features are the strongly shifted ^{29}Si resonances of the central silicon to higher fields and small $^1J(Si-C)$ coupling constants for the peripheral silicon atoms. Surprisingly, *systematic* changes are found only for ^{13}C and ^1H resonances. Perhaps they are related to the different extent of intramolecular $M\cdots CH_3$ interactions (see below).

The observed Raman bands of the crystalline compounds (Table 2) also show only small differences. Compared to the parent silane $HSi(SiMe_3)_3$: the symmetric Si–Si valence vibration $\nu_s(Si-Si)$ is shifted to a higher frequency, whereas the corresponding asymmetric vibration $\nu_{as}(Si-Si)$ is observed at a lower frequency, although the mean value is virtually the same for both types of compounds. These differences may arise from the more acute Si-Si-Si angles (101–105°) in the hypersilanide anions, leading to a reduction in coupling between the symmetric and asymmetric modes.

Table 1. NMR data of alkali metal hypersilanides.

Compound	$\delta(^1H)$	$\delta(^{13}C)$	$\delta(^{29}Si)$ $Si(SiMe_3)_3$	$\delta(^{29}Si)$ $Si(SiMe_3)_3$	$^1J(C-Si)$ [Hz]
$LiSi(SiMe_3)_3$ (**5**)	0.45	6.5	−8.9	−184.2	43.3
$NaSi(SiMe_3)_3$ (**1**)	0.45	6.7	−6.0	−179.8	40.2
$KSi(SiMe_3)_3$ (**2**)	0.53	7.4	−5.8	−185.7	38.8
$RbSi(SiMe_3)_3$ (**3**)	0.53	7.5	−5.6	−184.4	38.9
$CsSi(SiMe_3)_3$ (**4**)	0.47	7.9	−5.3	−179.4	38.6

Table 2. Raman lines of the alkali metal hypersilanides $MSi(SiMe_3)_3$ and hypersilane below 800 cm^{-1}.

Mode	Li	Na	K	Rb	Cs	H [28]
$\delta(Si-Si)$	119 s	120 s	124 s	120 ms	118 ms	135 w
$\rho(SiC_3)$	160 sh	161 sh	163 sh	162 sh	162 sh	–
$\rho(SiC_3)$	177 vs	180 vs	181 vs	180 vs	178 vs	162 vs
$\delta_{as}(SiC_3)$	224 w	–	–	–	–	218
$\delta(SiC_3)$ (+ $\nu_s(SiSi)$)	232 s	234 s	235 s	235 s	237 s	218 s
$\delta(SiC_3)$ + $\rho(SiC_3)$	256 s	278 s	277 s	276 s	275 s	273 w
$\nu_s(Li-Si)$?	294 w					
$\nu_s(SiSi)$ (+ $\delta(SiC_3)$)	371 ms	371 ms	371 ms	371 s	372 s	357 vs
$\nu_{as}(SiSi)$	433 m	433 m	434 m	432 m	432 ms	444 m
$\nu_s(SiC)$	628 ms	627 ms	627 ms	624 ms	626 ms	623 vs
$\nu_{as}(SiC)$	679 s	673 vs	670 s	668 vs	667 vs	685 s
$\rho(CH_3)$	748 ms	745 ms	744 m	745 s	746 s	743 m

  0947-6539/97/0309-1419 $ 17.50+.50/0

The similarity of the NMR and Raman spectra can be rationalized if it is assumed that there is predominantly ionic bonding throughout this series. This hypothesis is further supported by *ab initio* calculations on model systems. These reveal that the M–Si bonds possess only about ten percent covalent character (Table 3; Figures 1 and 2). The covalent contribution may be somewhat higher only in the case of lithium, or the more electronegative sodium. Interestingly, the ^{29}Si NMR spectra do not display the expected systematic dependence of the chemical shifts upon the metal present. This is presumably due to different interactions with the employed solvent, hexadeuterobenzene. Nothing definite is known about aggregation in solution, however, benzene forms solvates with the hypersilanides of potassium, rubidium, and cesium in the solid state, but not with the derivatives of lithium and sodium (see below).

Appropriate model systems, which are suitable for ab initio calculations at a modest level of theory, are the C_{2h} structures II of the $(MSiH_3)_2$ dimers (Figure 1). The calculated geometric

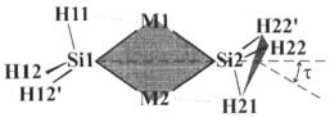

Figure 1. Isomer II of dimeric alkali metal trihydrosilanides (C_{2h} symmetry). The tilt angle τ is defined as the angle between the planes through the hydrogen atoms of a trihydrosilyl moiety and the Si1–Si2 vector.

parameters and charge distributions from natural population analysis (NPA) for these model compounds and for the corresponding monomers, $MSiH_3$, are listed in Tables 3a and 3b.

Table 3. Geometric parameters and NPA charges (Q):
a) In MP2-optimized $M_2(SiH_3)_2$ structures (II) (values for the idealized structures I in parentheses).

M	Li	Na	K	Rb	Cs
M1–Si1	260.5 (264.0)	301.2 (298.2)	340.2 (337.4)	356.5 (351.1)	370.4 (367.5)
M1–Si2	258.3	290.6	337.4	355.2	374.4
M1–M2	278.3 (241.6)	337.1 (299.1)	415.8 (394.1)	447.3 (428.9)	484.8 (473.8)
Si1–Si2	437.8 (469.4)	486.5 (517.9)	535.0 (547.9)	553.6 (561.1)	565.4 (562.0)
Si1–H11	155.5 (150.1)	154.3 (150.6)	153.6 (151.3)	153.3 (151.6)	153.3 (151.9)
Si1–H12	149.7	150.2	150.8	151.1	151.4
M1–H11	184.9	222.0	260.6	277.7	295.9
M1-Si1-M2	64.9 (51.5)	69.4 (60.2)	75.7 (71.5)	77.9 (74.8)	81.2 (80.3)
Si1-M1-Si2	115.1 (125.5)	110.6 (119.8)	104.3 (108.5)	102.1 (105.2)	98.8 (99.7)
H12-Si1-H12'	103.5 (102.6)	102.2 (101.1)	100.2 (99.4)	99.8 (99.0)	99.0 (98.4)
H11-Si1-H12	97.2	97.3	97.0	97.0	96.9
Si2···Si1-H11	76.7 (115.7)	79.4 (116.7)	84.6 (118.3)	86.6 (118.6)	90.8 (119.0)
Si2···Si1-H12	128.2	128.9	129.6	129.7	129.5
Q(M)	+0.77	+0.82	+0.89	+0.92	+0.93
Q(Si)	−0.20	−0.23	−0.29	−0.30	−0.32
Q(H11)	−0.28	−0.27	−0.26	−0.26	−0.25
Q(H12)	−0.15	−0.16	−0.17	−0.18	−0.18

b) In MP2-optimized $MSiH_3$ structures.

M	Li	Na	K	Rb	Cs
M–Si	248.7	277.6	319.9	336.3	354.1
Si–H1	150.1	150.1	150.8	150.9	151.2
H1-Si-H2	102.7	102.8	101.0	100.7	100.0
M-Si-H1	115.5	115.5	117.0	117.2	117.8
Q(M)	+0.76	+0.69	+0.79	+0.81	+0.85
Q(Si)	−0.25	−0.16	−0.24	−0.25	−0.28
Q(H)	−0.17	−0.18	−0.18	−0.19	−0.19

In the dimers, the silyl group is strongly tilted with respect to the Si–Si vector (demonstrated by the angle τ between the normal vector on the H_3 plane of the SiH_3 group and the Si–Si bond vector). This is caused by an interaction of one of the partially negatively charged hydrogen atoms on each silicon with the alkali metal cation. Comparable structural features are observed for some of the alkali metal hypersilanide dimers. As will be detailed below, the partially negatively charged methyl groups of the hypersilyl substituent behave similarly, in that they also coordinate the metal cations. In some cases, a substantial tilting of the whole hypersilyl group from the corresponding Si–Si vector is observed (Table 4). The charge distribution, derived from natural population analysis (NPA) (Tables 3), indicates that the bonds are already mainly ionic in the monomers and even more so in the dimers. A similar conclusion was made a few years ago by Schleyer et al. from calculations on $LiSiH_3$ and $NaSiH_3$.[11]

A closer inspection of the hypersurface reveals that the C_{2h} structure II is not the only local minimum—it is not even the global one. However, all the minima found are close in energy and do reflect the variety of alkali metal hypersilanide structures found experimentally. The global minimum is represented by a second C_{2h} structure, III. It is comprised of four hydrogen atoms in close contact with the alkali metal cations. Here, as in most of the investigated $M_2(SiH_3)_2$ isomers (II to IX), the silyl groups are tilted even more markedly by the obviously strong M···H interactions, leading to extremely divergent M–Si bond lengths (shown for the isomers of $Rb_2(SiH_3)_2$ in Figure 2) compared to the idealized structure (I), which has equal Rb–Si bonds and local D_{3d} symmetry for the $H_3Si\cdot\cdot SiH_3$ moiety. The energy gained by the M–H interactions is almost additive and can be estimated to be about 7–8 kJ mol^{-1} per Rb-H-Si bridge. Notable exceptions are the isomers VIII and IX: as a consequence of steric restrictions, the M–H distances are rather long and the interaction energy is considerably smaller (<1.5 kJ mol^{-1}). The interaction energy corresponding to the other M-H-Si bridges has been determined to be approximately 18 (Li), 14 (Na), 9 (K), and 5 (Cs) kJ mol^{-1}.

The hypersilyl ligand contains a couple of more electronegative carbon atoms, thus producing a higher group electronegativity than the small trihydrosilyl substituent used in these calculations. This may lead to an even more ionic bond. Since the alkali metal hypersilanide dimers observed experimentally are far too big for reliable calculations, the charge distribution was calculated for the monomeric lithium hypersilanide at the Hartree–Fock level with medium-sized basis sets and then compared to Li–SiH_3 calculated at the same level. Indeed, the charge of +0.80 on the lithium atom in lithium hypersilanide is higher than the +0.76 calculated for $LiSiH_3$. Furthermore, it is interesting to compare the charge distribution within the hypersilyl group with that in the related supersilyl ligand ($(t$Bu$)_3$Si-), since the alkali metal derivatives containing the latter group are much more reactive than hypersilanides towards weak bases such as benzene or toluene (as are most of the other known silanides).[12a] Calculations—again at the Hartree–Fock level—reveal that the central silicon atom within the hypersilyl group

0947-6539/97/0309-1420 $ 17.50+.50/0 *Chem. Eur. J.* **1997**, *3*, No. 9

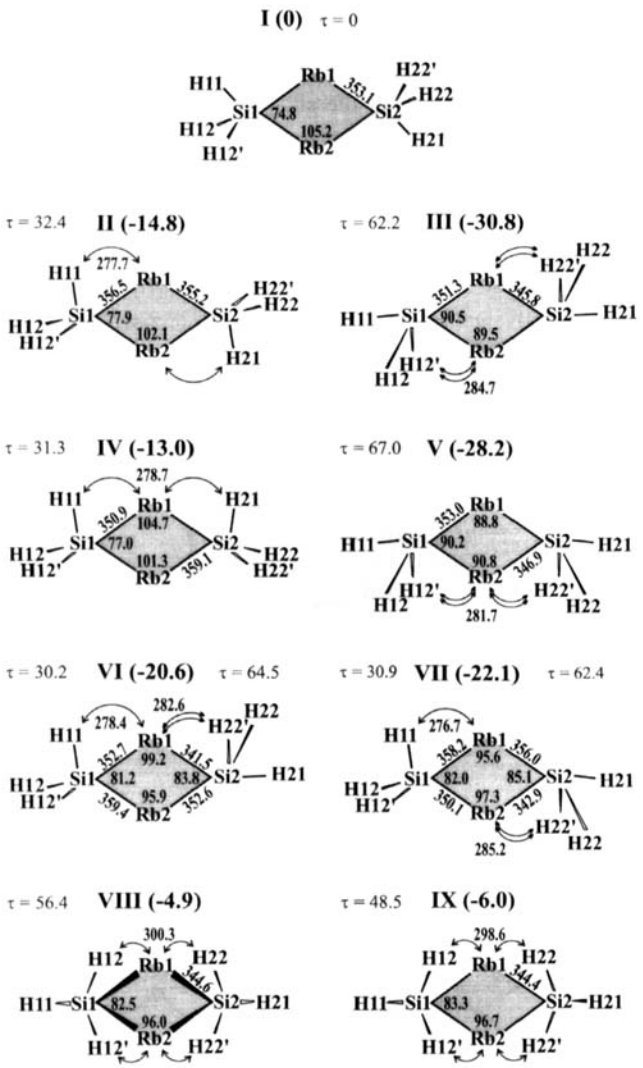

Figure 2. Calculated structures of the isomers I–IX of dimeric rubidium trihydrosilanide, with selected distances [pm] and angles [°]. The relative energies [kJ mol^{-1}] are given in parentheses. The tilt angle τ is defined as in Figure 1.

bears a relatively high negative charge, as do the peripheral carbon atoms. Whereas in the supersilyl group, the charge is nearly equally distributed amongst all carbon atoms (Figure 3). The alkali metal cation is bonded more tightly to the central

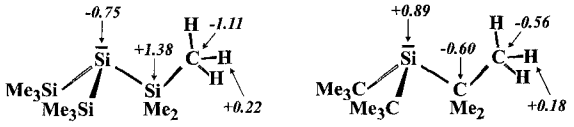

Figure 3. Charge distributions within the hypersilanide and supersilanide anions derived from natural population analysis (NPA). Mean values are given for charges on the hydrogen atoms.

silicon in the hypersilyl ligand, as it is additionally chelated and held in place by the more negatively charged peripheral methyl groups. Thus, the overall effect is a blocking of the nucleophilic center. Finally, an interesting result from the population analyses performed on K, Rb, and Cs compounds should be mentioned here: the small amount of electron density remaining at the alkali metal is located in nearly equal proportions in s and d(!) orbitals, whereas the contribution of p orbitals is negligible. This perhaps reflects the fact that ns and $(n-1)$d orbitals are of very similar energy in these elements, particularly if the effective charge of the nuclei is raised by (partial) ionization.

Addition of π or σ donors to suspensions or solutions of the alkali metal hypersilanides in pentane frequently leads to the formation of colored solutions, from which crystalline solvates can be isolated in some cases. However, with certain potential donors, such as phenanthrene, diphenylacetylene, and bipyridine, reactions such as deprotonation, reduction, and addition can take place, and they usually lead to complicated mixtures of products.

Lithium, sodium, and potassium hypersilanides form solvates with σ donors bearing oxygen (e.g. tetrahydrofuran (THF), dimethoxyethane (DME), diethyl ether) or nitrogen (e.g. tetramethylethylenediamine (TMEDA), pentamethyldiethylenetriamine (PMDTA)) from which, in most cases, the donor molecule cannot be removed without decomposition. In contrast, some solvates of rubidium and cesium hypersilanides, containing such donors, are more labile. For example, diethyl ether and dimethoxyethane are easily replaced by solvent molecules when heated in toluene. This ligand may then be removed in a vacuum to yield the solvent-free compound. A closer look at the solid-state structures of these solvent-free derivatives reveals that, in spite of the missing solvent molecules, these compounds are not really free of donor ligands. As will be discussed in detail below, methyl groups of the hypersilyl ligand may act as intra- and intermolecular donors.

Molecular structures of solvent-free 1a and 2a, and the inclusion compound 1b: The molecular structures of **1a** (Figure 4), **1b** (Figure 5), and **2a** (Figure 6) were obtained by X-ray diffraction

$[MSi(SiMe_3)_3]_2$ **1a** (M = Na); **2a** (M = K)

$[NaSi(SiMe_3)_3]_2 \cdot$benzene **1b**

at −100 °C of single crystals obtained by recrystallization from n-pentane (**1a**, **1b**) or an n-pentane/toluene mixture (**2a**). The

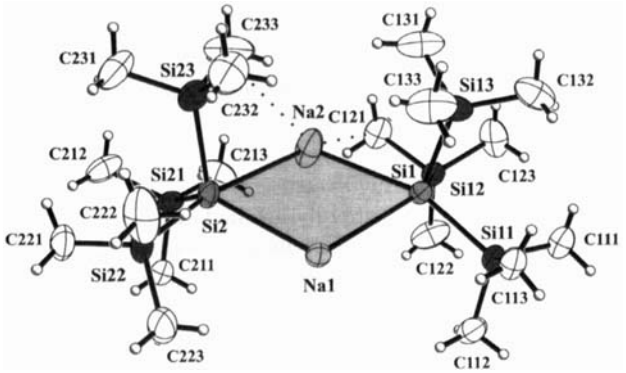

Figure 4. Molecular structure of one of the two independent molecules in **1a** (ellipsoids at the 30% probability level). Dotted lines indicate short intramolecular Na···CH_3 contacts. Selected intramolecular distances [pm] and angles [°]: Na1–Si1 302.5(2), Na1–Si2 299.3(2), Na2–Si1 298.3(2), Na2–Si2 294.1(2), Na···Na 316.9(2), Si1-Na1-Si2 113.78(5), Si1-Na2-Si2 116.64(6), Na1-Si1-Na2 63.66(5), Na1-Si2-Na2 64.55(5).

  0947-6539/97/0309-1421 $ 17.50+.50/0

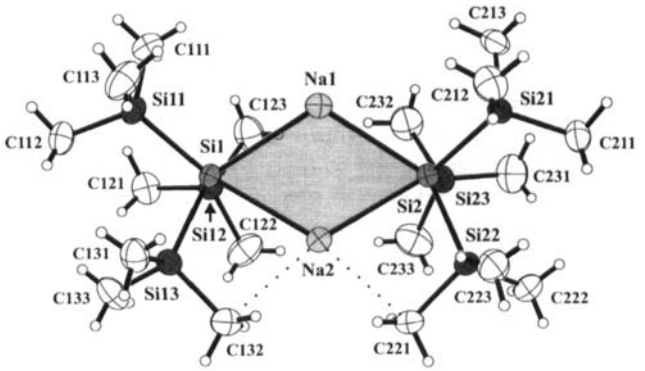

Figure 5. The molecular structure of **1b** (ellipsoids at the 30% probability level). Dotted lines indicate short intramolecular Na···CH_3 contacts. Selected intramolecular distances [pm] and angles [°]: Na1–Si1 304.9(1), Na1–Si2 304.6(1), Na2–Si1 299.6(1), Na2–Si2 299.8(2), Na···Na 311.1(2), Si1-Na1-Si2 113.67(4), Si1-Na2-Si2 116.70(4), Na1-Si1-Na2 61.94(3), Na1-Si2-Na2 61.96(3).

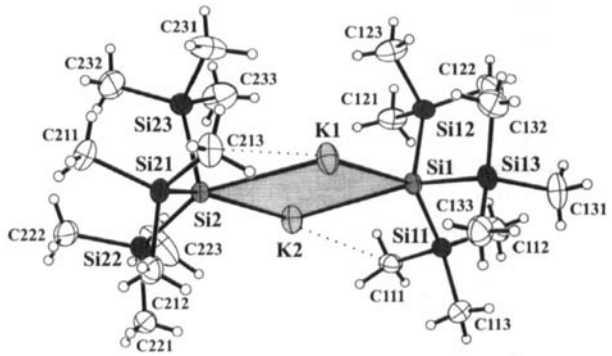

Figure 6. Molecular structure of **2a** (ellipsoids at the 30% probability level). Dotted lines indicate short intramolecular K···CH_3 contacts. Selected intramolecular distances [pm] and angles [°]: K1–Si1 341.66(9), K1–Si2 341.6(1), K2–Si1 336.8(1), K2–Si2 337.66(9), K···K 404.86(9), Si1-K1-Si2 105.70(2), Si1-K2-Si2 107.72(2), K1-Si1-K2 73.28(2), K1-Si2-K2 73.17(2).

structure of **1a** comprises two symmetry-independent molecules, one of which shows a statistical disordering of the sodium atoms. The discussion therefore concentrates on the well-ordered structural unit. The common structural feature is a four-membered M_2Si_2 ring, virtually planar in **2a** and slightly bent in **1a** and **1b** (Table 4). Similar structures were found for both forms of solvent-free lithium hypersilanide (**5**) (Figures 7 and 9a)[1b] and most of the investigated solvates of the heavier analogues (see below and in ref. [1a]). In the latter compounds pronounced ring-folding occurs, due to additional unsymmetrical coordination by solvent molecules. The analogous alkali metal supersilanides ($M^ISi(tBu)_3$; M = Li, Na) display very similar structures.[8, 12a] In contrast, the related alkali metal derivatives of tris(trimethylsilyl)*methane* show different structural motifs:[13] the tris(trimethylsilyl)methanide anion contains an almost planar central carbon, which is coordinated in a nearly linear fashion in its potassium and rubidium derivatives. Moreover, these compounds do *not* consist of discrete molecules, but are polymerized to infinite chains.

The coordination polyhedron around the central silicon atom of the hypersilyl ligand exhibits distinct differences on changing the bonded metal from lithium to sodium and potassium (Figure 8). Within the low-temperature phase of **5a** a mono-

$[LiSi(SiMe_3)_3]_2$ **5a**

capped tetrahedron is found (Figure 7, 8),[1b] whereas for **1b** as well as for **2a** [and for $(\mathbf{4})_2 \cdot THF$ (see below)] the coordination geometries around Si1 and Si2 are more accurately described as tetragonal pyramids, with the alkali metal atoms lying in the basal planes. The Na_2Si_8 skeleton of **1a** possesses a different geometry, which is best described in terms of two $NaSiSi_3$ tetrahedra linked by a common sodium atom (Na1), which are both capped by the second sodium (Na2). A further possible coordination geometry, the trigonal bipyramid, was observed for the toluene solvates of rubidium and cesium hypersilanide, **3a** and **4a**, respectively (Table 4).[1a] The different coordination ge-

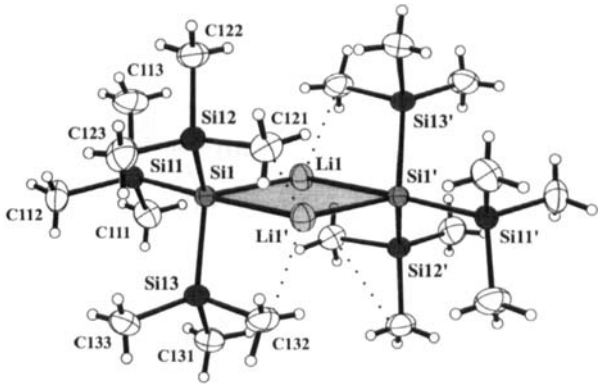

Figure 7. Molecular structure of **5a** at −100 °C (ellipsoids at the 30% probability level). Dotted lines indicate short intramolecular Li···CH_3 contacts. Selected intramolecular distances [pm] and angles [°]: Li1–Si1 258.7(4), Li1–Si1′ 260.1(4), Li···Li′ 275.7(7), Si1-Li1-Si1′ 115.8(1), Li1-Si1-Li1′ 64.2(1).

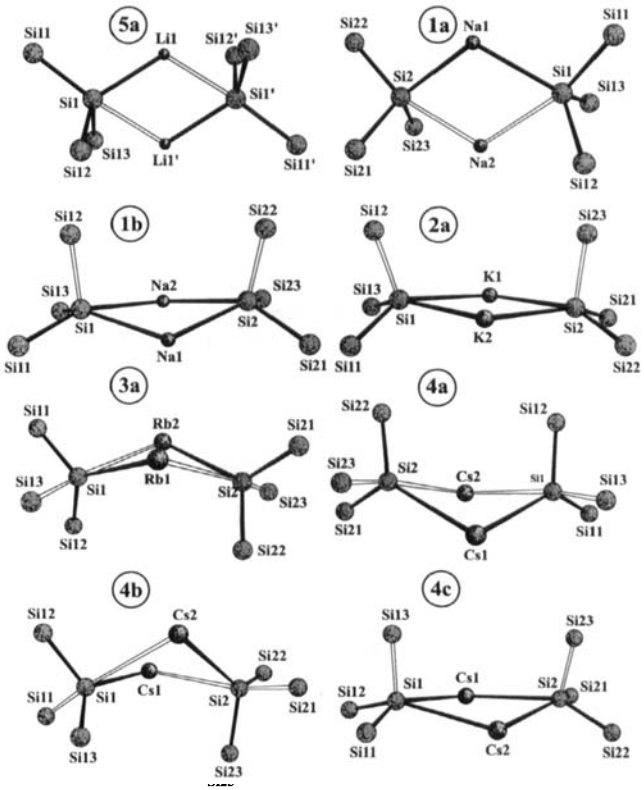

Figure 8. Coordination geometry around the central silicon atoms in **5a**, **1a**, **1b**, **2a**, **3a**, **4a**, **4b**, and **4c**. Axial bonds in trigonal bipyramids, the bond to the apical atom in tetragonal pyramids, and the bond to the capping atom in capped tetrahedra are depicted as open lines (=).

0947-6539/97/0309-1422 $ 17.50+.50/0

Table 4. Structural parameters in alkali metal hypersilanides [a].

	M	CN [b]	M–Si	M···M	Si···Si	Si-M-Si	M-Si-M	τ [c]	θ [d]	Si–Si (mean)	Si-Si-Si (mean)
α-(**5**)$_2$ (**5a**)	Li	2Si+2C	259; 260	276	440	115.8	64.2	30.9	0.0	233.9	107.5
β-(**5**)$_2$ (**5b**)	Li	2Si+1C; 2Si	262–270	265	462	118.2; 122.5	59.4; 59.8	10.1; 23.1	4.5	233.4	105.1
5·3THF [21]	Li	1Si+3O	264	–		–	–	–	–	233.0	102.4
(**5**)$_2$·3DME [23]	Li	1Si+3O	263	–		–	–	–	–	234	104
(**1**)$_2$ (**1a**)	Na	2Si+2C	294–303	317	504	113.8; 116.6	63.7; 64.5	17.4; 19.2	10.0	234.0	103.3
(**1**)$_2$·benzene (**1b**)	Na	2Si+2C	300 305	311	510	113.7; 116.7	61.9; 62.0	17.2; 25.8	20.1	234.4	102.5
(**2**)$_2$ (**2a**)	K	2Si+3C	337–342	405	545	105.7; 107.7	73.2; 73.3	7.8; 19.7	3.4	233.8	102.3
2·(benzene)$_3$ (**2b**)	K	1Si+3A	332–335	–					–	233.6	101.5
(**3**)$_2$·toluene (**3a**)	Rb	2Si; 2Si+1A [e]	352–362	431	534	95.4; 98.3	74.2; 74.3	19.4; 26.1	40.5	233.5	102.4
(**4**)$_2$·(toluene)$_3$ (**4a**)	Cs	2Si+1A; 2Si+2A [e]	377–385	492	551	92.0; 93.6	80.4; 80.9	18.7; 27.2	36.5	234.4	100.9
(**4**)$_2$·biphen·(pentane)$_{0.5}$ (**4b**)	Cs	2Si+1A; 2Si [e]	368–381	464	538	90.5; 93.0	75.7; 77.1	18.7; 32.2	48.0	233.5	101.2
(**4**)$_2$·THF (**4c**)	Cs	2Si+1O [e]	367–373	420	604	108.7 109.8	69.0	20.7; 20.8	16.4	233.2	102.3

[a] Several independent values are separated by a semicolon, ranges by a dash. [b] Coordination numbers. Si: silicon; C: methyl group; O: oxygen; A: aromatic ring. [c] Angle τ defined as in Figure 1. [d] Interplanar angle θ: M-Si-M/M-Si-M. [e] Several additional contacts to methyl groups.

ometries are caused by different intra- and intermolecular interactions and different radii of the alkali metal cations as described in detail below.

The mean Na–Si and K–Si distances of 298.6 (**1a**), 302.2 (**1b**), and 339.5 pm (**2a**) (Table 4) are in excellent agreement with the sum of the covalent radii of the alkali metals derived from X-ray data of other organometallic derivatives (Na: 183 pm; K: 221 pm[14]) and the value for silicon (117 pm), although deviations occur which correlate to differences in the coordination sphere of the cation. Within solvates such as **2b** (Table 4) or the [K([18]crown-6)$^+$]$_2$[$C_4Me_4Si^{2-}$],[12b] the K–Si bonds are even shorter than those found in the solvent-free compound **2a**. Similarly, the Na–Si bonds in the monomeric PMDETA and THF solvates of sodium supersilanide [(*t*Bu)$_3$SiNa·(THF)$_2$] (297 and 292 pm, respectively)[12a] are much shorter than that in the corresponding dimeric solvent-free compound [(*t*Bu)$_3$SiNa]$_2$ (307 pm).[7, 12a] The coordination numbers of the potassium cation and the silanide anion are both higher in the related structures of $KSiH_3$, leading to longer K–Si distances (>355 pm for the ordered phase β-$KSiH_3$[7c]). Crystalline $NaSiH_3$ has not yet been reported (although it is known in solution[15a]); however, a Na···SiH_3 fragment has been structurally characterized as part of a mixed silanide/alcoholate complex by Sundermayer et al. In this compound the sodium ion is not directly bonded to silicon, but is coordinated to the three hydridic hydrogen atoms of the SiH_3 moiety.[15b] Nevertheless, the observed Na–Si distance of 305 pm is only marginally longer than the mean Na–Si distances for **1a** and **1b**. Calculations reveal much shorter Na–Si bonds [277.5 pm[15b]; 277.6 pm (this work)] for the unsolvated monomeric Na–SiH_3 unit, as would be expected for the higher bond order (bo = 1 vs. ca. 0.5 in the dimers).

Very acute Si-Si-Si angles and short Si–Si bonds were found to be a common feature in all alkali metal hypersilanides (Table 5). This is indicative for extensive charge transfer from the metal to the ligand and leads to steric stress within the substituent. The trimethylsilyl groups are tilted outwards to produce Si-Si-C angles of up to 120° (in **2a**).

All dimers show very close intramolecular contacts between the alkali metal atoms within the M_2Si_2 ring (Na···Na: 317 (**1a**), 311 (**1b**); K···K: 405 pm (**2a**)), which are much shorter than in the solid-state structure of the corresponding metal. Even closer contacts are found in the lithium and sodium supersilanides: Li···Li and Na···Na contacts as short as 240 and 286 pm, respectively, are reported.[7, 12a] However this, as in other small-ring systems, is not necessarily the result of an attraction, but a consequence of the geometric restrictions in such small rings.

Crystal Structures: The peculiarities of the molecular as well as the crystal structures of hypersilyl derivatives of lithium (α-(**5**)$_2$ and β-(**5**)$_2$), sodium (**1a** and **1b**), and potassium (**2a**) originate from the differing sizes of the cations, and as a further consequence, from the differing extent of interactions between the alkali metal ion and trimethylsilyl groups of the same or of neighboring molecules. While the low-temperature α-form of lithium hypersilanide (**5a**) consists of isolated dimers (Figure 7), in all the other hypersilanides two such [$MSi(SiMe_3)_3$]$_2$ dimers form aggregates—"super-dimers"—through short M···CH_3 links (Figures 9). In high-temperature β-(**5**)$_2$ (**5b**) only van der Waals interactions are observed between these super-dimers, while in the case of the larger sodium cation further aggregation leads to infinite chains, which are stacked in different ways in **1a** and **1b** (Figures 10 and 11), respectively. The structure of potassium hypersilanide **2a** consists of chains with similar stacking as in **1b**, with additional M···CH_3 interactions due to the larger size of potassium (Figure 12). Thus, a three-dimensional network is formed resulting in low solubility of **2a** in nonpolar solvents.

M···CH_3 interactions are present not only between, but also *within* the dimers. Although they seem to be weaker (longer), at least for M = Na and K, they are perhaps partly responsible for the rather low reactivity towards solvent molecules as they chelate the alkali metal cation, holding it in place and thus blocking the nucleophilic silicon center. Such M···CH_3 interactions are often referred to as "agostic", although this expression was originally coined by Green to describe the three-center M···H···C bonds in transition metal compounds.[16] In hypersilanides, however, as in many other cases where a main group metal ion with low charge and coordination number interacts with trimethylsilyl or similar groups[17] (e.g. in ref. [13,14]), I believe that the interaction is best described by a different model described by two components:

1) a purely electrostatic interaction of the M–Si and Si–CH_3 dipoles, which are often aligned in a antiparallel "side-on"

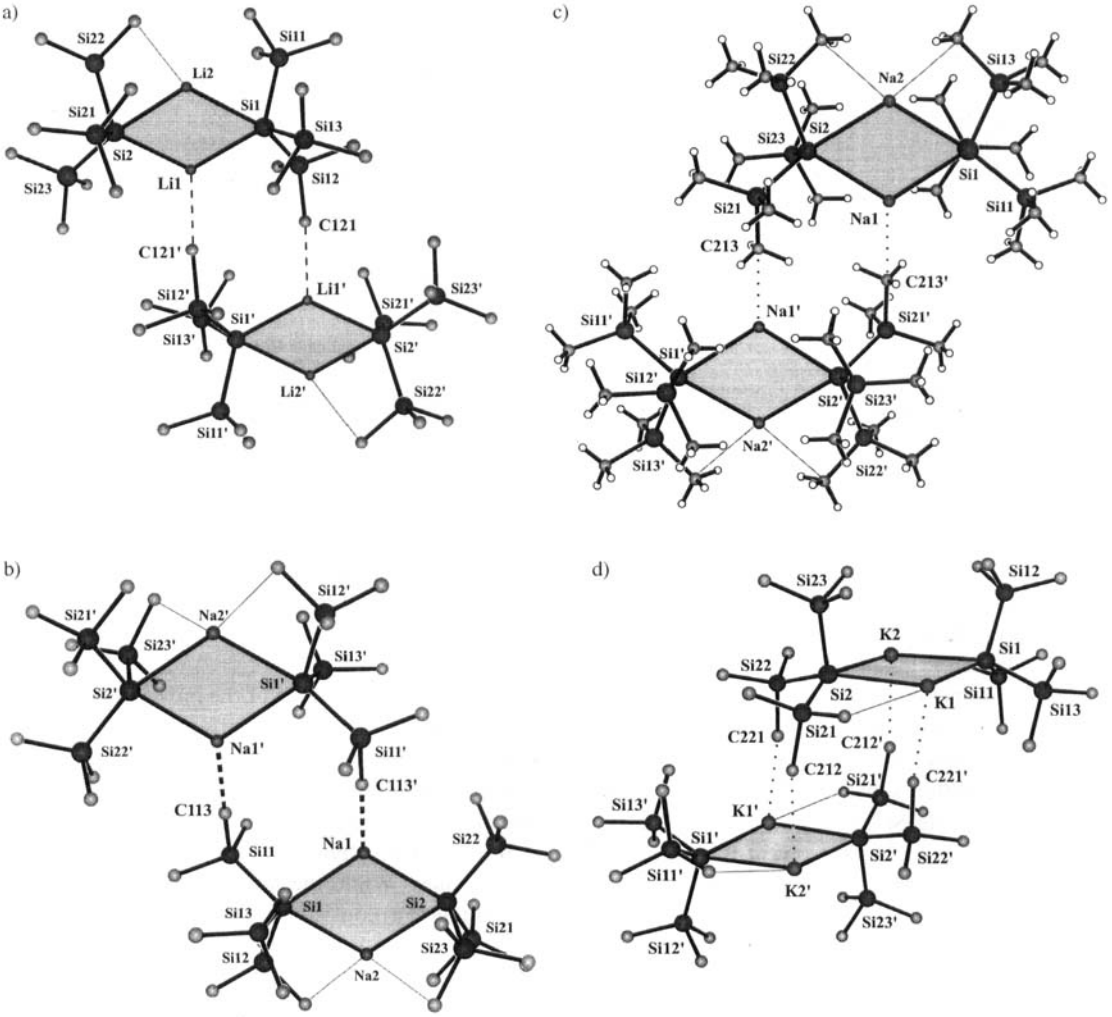

Figure 9. Formation of "super-dimers" in alkali metal hypersilanides. Dotted lines indicate short intermolecular M···CH_3 contacts. M–C distances are listed in Table 5. a) **5b**; b) **1a**; c) **1b**; d) **2a**.

fashion for the intramolecular case and in a parallel "head-to-tail" fashion in the intermolecular case (Figure 13a);

2) a donor–acceptor interaction between C–H bonding electron pairs and the electron-deficient metal cation (Figure 13b).

The latter is always more advantageous for intermolecular interactions, because there are three C–H bonds available, whereas for steric reasons only two C–H bonds can serve as *intra*molecular donors. Therefore, the shortest M···C contacts observed in the alkali metal hypersilanides (Table 5) are intermolecular, with few exceptions—for example, in the lithium derivatives **5a** and **5b** the small lithium cation is hardly accessible for intermolecular interactions. Note that within the molecular structures of $[LiSi(tBu)_3]_2$ and $[NaSi(tBu)_3]_2$ only intramolecular M···CH_3 interactions occur. As a result of the virtually *nonpolar* nature of the C–CH_3 bond, significantly longer M–C distances are observed (254 and 313 pm, respectively).[7, 12a]

There seems to be a (small) influence of these contacts on the lengths of the Si–C bonds. These are lengthened by some 2 pm (2%) in **1a**, **1b**, and **2a** compared to other Si–C bonds where no such contacts exist, although the standard deviations of 0.3–0.6 pm preclude any definitive statement. In the lithium derivative **5a**, however, the Si–C bonds *are* significantly lengthened by some 2.5% (191 vs. 184–186 pm).

Solvent-free 3 and 4: Unfortunately, **3** and **4** have not yet been obtained as single crystals since they are insoluble in weakly

$RbSi(SiMe_3)_3$ **3**

$CsSi(SiMe_3)_3$ **4**

coordinating hydrocarbons such as pentane or heptane. Although dimeric building blocks similar to those in the crystal structures of lithium, sodium, and potassium hypersilanides are probable, the larger radii of rubidium and cesium certainly lead to a more extensive linking through metal–methyl bridges than already observed for **2a**. Dimers are definitely found in a number of solvates containing aromatic hydrocarbons or ethers as donor ligands.

Hitherto the only exceptions in which the dimeric unit is cleaved by hydrocarbons are the benzene solvates. This has been proved unambiguously by X-ray diffraction only for the bright yellow potassium derivative **2**·(benzene)$_3$ (**2b**). The cesium and rubidium hypersilanides **3** and **4**, however, also crystallize from

0947-6539/97/0309-1424 $ 17.50+.50/0 *Chem. Eur. J.* **1997**, *3*, No. 9

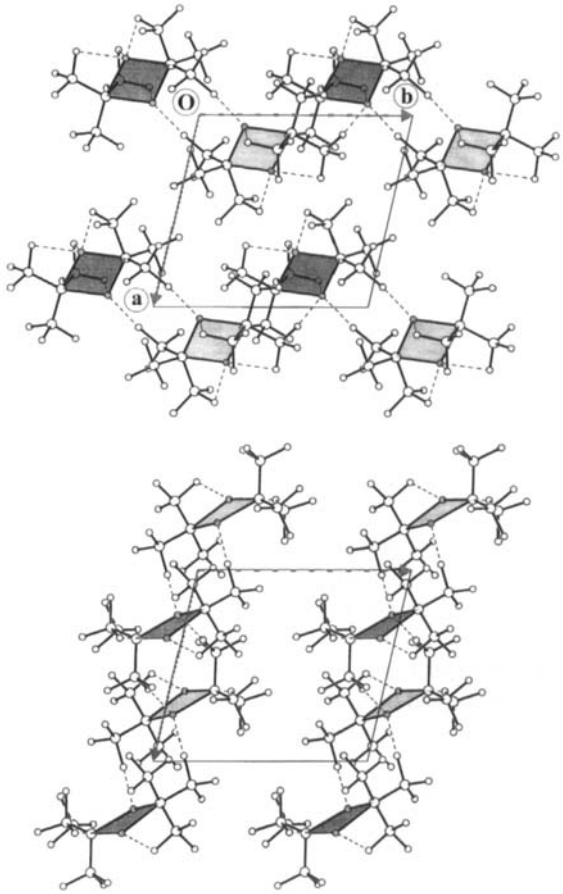

Figure 10. Further polymerization of the super-dimers to infinite chains through $M\cdots CH_3$ interactions in **1a**. The two independent types of polymer chains form sheets parallel to (001) in different levels of the unit cell, the chains are orientated parallel to [100] and [010], respectively. Dotted lines indicate short intra- and intermolecular $Na\cdots CH_3$ contacts.

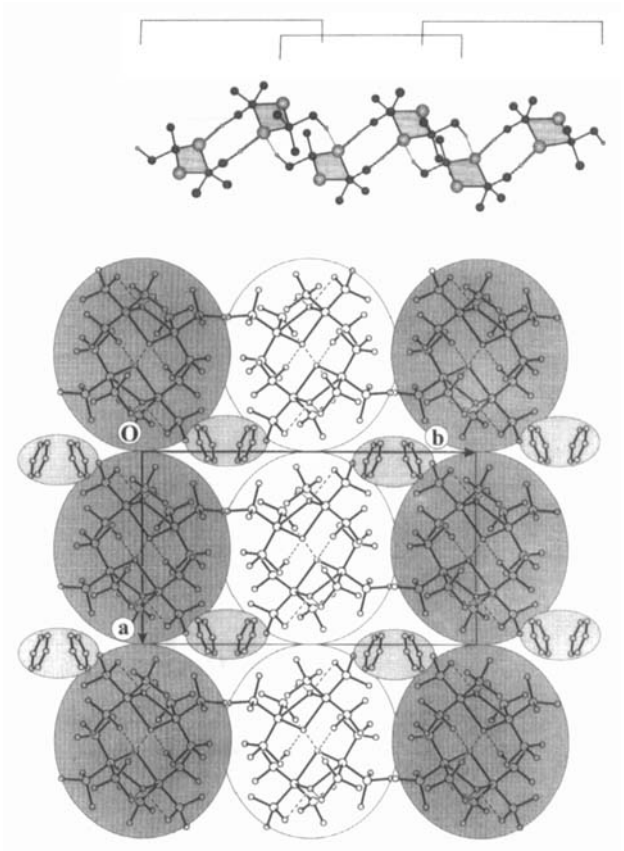

Figure 11. Top: Further polymerization of the super-dimers to infinite chains through $Na\cdots CH_3$ interactions in **1b**. The positions of the super-dimers (Figure 9c) are indicated by brackets. Only those carbon atoms are displayed which are involved in close intermolecular $Na\cdots CH_3$ contacts. Bottom: Packing of the coordination polymers in **1b**. The benzene molecules are located in channels between the polymer rods.

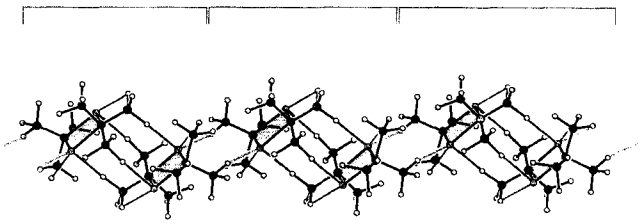

Figure 12. Further polymerization of the super-dimers to infinite chains through $K\cdots CH_3$ interactions in **1b**. The positions of the super-dimers (Figure 9d) are indicated by parentheses.

pentane/benzene solutions as bright yellow crystals and, according to their NMR spectra, also contain three benzene molecules per hypersilanide moiety. Unfortunately, the investigated specimens were twinned and could not be investigated by X-ray diffraction so far. Compounds **3** and **4** form crystalline toluene solvates $(\mathbf{3})_2\cdot$toluene (**3a**) and $(\mathbf{4})_2\cdot(\text{toluene})_3$ (**4a**),[1a] whereas the toluene solvate of potassium hypersilanide (**2b**), which has the same stoichiometry and probably a similar structure as the rubidium derivative, decomposes below $-10\,^{\circ}C$.

Benzene solvate 2b: The (twinned) bright yellow crystals of **2b** contain three independent monomeric molecules (A, B, C) all

$KSi(SiMe_3)_3\cdot(benzene)_3$ **2b**

displaying crystallographic C_3 symmetry (shown for A in Figure 14). These molecules are characterized by a short K–Si bond of about 334 pm, acute Si-Si-Si angles of 101°, and nearly ideal η^6-coordination of the benzene ligands. The K–arene distances (302–308 pm) lie in the same range as in other complexes of this type (examples in ref. [14]). The alkali metal ion seems to be coordinatively saturated by one hypersilanide ligand and three benzene molecules, since, in contrast to all other hypersilanides mentioned here, no short $M\cdots CH_3$ contact (neither intra- nor intermolecular) is found and thus no aggregation is observed for the solid state. A very similar structure had been observed for the corresponding tris(benzene) solvate of potassium supersilanide, $(t\text{Bu})_3\text{SiK}\cdot(\text{benzene})_3$.[12a] The observed K–Si and $K-C_{arom}$ distances in the supersilanide, however, were determined to be 338 and 348–352 pm, respectively, which is significantly longer than in **2b**. This difference is probably mainly due to steric effects.

In the crystal structure the polar monomers are lined up in a head-to-tail fashion, leading to chains of crystallographically related molecules ($\cdots A\cdots A\cdots A\cdots$ or $\cdots B\cdots B\cdots B\cdots$ or $\cdots C\cdots C\cdots C\cdots$). These chains are orientated parallel to one another and to the lattice vector c in such a way that a pseudorhombohedral lattice is formed.

Table 5. Short $M\cdots CH_3$ distances and corresponding $M\cdots C$–Si angles in alkali metal hypersilanides.

	M	Intramolecular M···C	Intramolecular M···C-Si	Intermolecular M···C	Intermolecular M···C-Si		M	Intramolecular M···C	Intramolecular M···C-Si	Intermolecular M···C	Intermolecular M···C-Si
α-$(5)_2$ (**5a**)	Li	240	87.2			$(4)_2\cdot(\text{toluene})_3$ (**4a**)	Cs	371	101		
		244	87.1					374	102		
β-$(5)_2$ (**5b**)	Li	270	84	249	171			384	95		
		276	87					392	84		
$(1)_2$ (**1a**)	Na	285	92	280	176	$(4)_2\cdot$biphen $\cdot(\text{pentane})_{0.5}$ (**4b**)	Cs	363	102	378	153
		305	87	286	167			365	101	387	155
$(1)_2\cdot$benzene (**1b**)	Na	285	91	276	173			384	92		
		288	92	299	165			385	95		
$(2)_2$ (**2a**)	K	334	95	325	173			389	92		
		341	96	332	170	$(4)_2\cdot$THF (**4c**)	Cs	372	100	366	154
				333	166			375	98	371	152
				333	163					373	160
$(3)_2\cdot$toluene (**3a**)	Rb	344	94	337	177					380	111
		359	102	351	153						
		362	98	360	154						

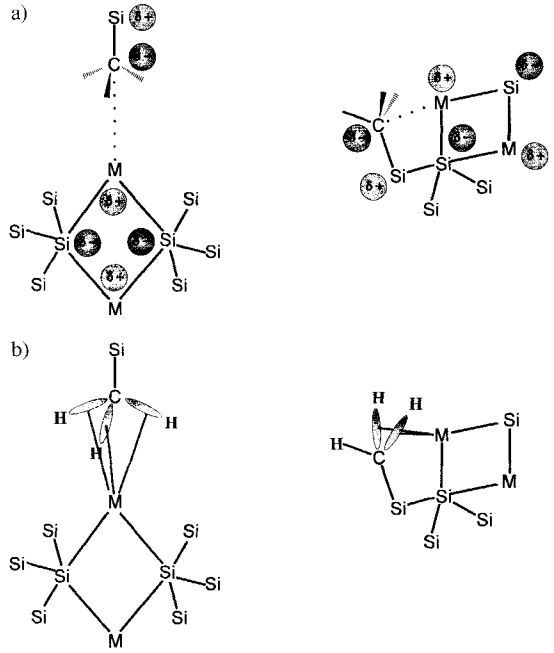

Figure 13. Inter- and intramolecular $M\cdots CH_3$ interactions in alkali metal hypersilanides: a) Dipole–ion component; b) C–H donor/M^+–acceptor component.

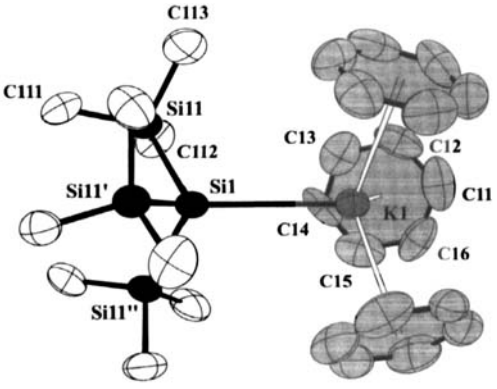

Figure 14. Molecular structure of one of the three independent molecules in **2b** (ellipsoids at the 50% probability level). Selected intramolecular distances [pm] and angles [°]: K1–Si1 335.2(4), K–C11 348(1), K–C12 342(1), K–C13 331(1), K–C14 328.3(9), K–C15 332(1), K–C16 339(1), K1–centroid 309, K1-Si1-Si11 116.93(8), Si11-Si1-Si11' 101.1(1), Si1-K1-centroid 105.8.

At first sight, the structure of **2b** looks very similar to that of the related tris(benzene) complex of cesium tris(trimethylsilyl)methanide.[13b] However, the methanide exhibits very *obtuse* Si-C-Si angles (117°) at the central carbon atom, in contrast to the very *acute* Si-Si-Si angles within the silanide **2b**. This difference can be rationalized by the more effective sp^2 hybridization of carbon and a very diffuse p-type orbital bearing the negative charge.

In the toluene solvates **3a** and **4a**,[1a] dimeric M_2Si_2 units are also present, which are no longer planar but strongly bent

$[RbSi(SiMe_3)_3]_2\cdot$toluene **3a**

$[CsSi(SiMe_3)_3]_2\cdot(\text{toluene})_3$ **4a**

(Figure 15; Table 4). Differences in the molecular and crystal structures are easily rationalized by the influence of different cation radii. Whereas the smaller rubidium permits the addition of only one toluene per rubidium hypersilanide dimer, there is enough space for three molecules of toluene in the cesium derivative. However, this prohibits the occurrence of intermolecular $Cs\cdots CH_3$ interactions and leads to isolated molecular units in **4a**, whereas the rubidium hypersilanide dimers in **3a** are extensively interconnected by $Rb\cdots CH_3$ links forming a three-dimensional network.

The solvate 4b: Addition of biphenylene to a suspension of cesium hypersilanide in pentane produced a pale yellow solution, which on cooling to −60 °C gave pale yellow crystals of **4b.** Rubidium hypersilanide also dissolves in pentane in the presence of biphenylene, however, crystals of a corresponding solvate have not yet been obtained.

$(4)_2\cdot$biphen$\cdot(\text{pentane})_{0.5}$ **4b**

Once again, a $[CsSi(SiMe_3)_3]_2$ dimer with a bent Cs_2Si_2 skeleton is found (Figure 16, top). Biphenylene, which for electronic reasons is expected to be a much weaker donor than toluene, acts as a bridging ligand here. One phenyl ring are nearly η^6-coordinated to Cs2; the observed $Cs\cdots C_{arom}$ distances is significantly longer than in the toluene solvate **4a**. The second phenyl ring acts as a η^1-donor to the Cs1 atom of a neighboring dimer. This coordination is best described as the coordination of a C–H bond to Cs1 (Figure 16, bottom). Additionally, there are intra- and intermolecular $Cs\cdots CH_3$ interactions with the tri-

0947-6539/97/0309-1426 $ 17.50+.50/0 *Chem. Eur. J.* **1997**, *3*, No. 9

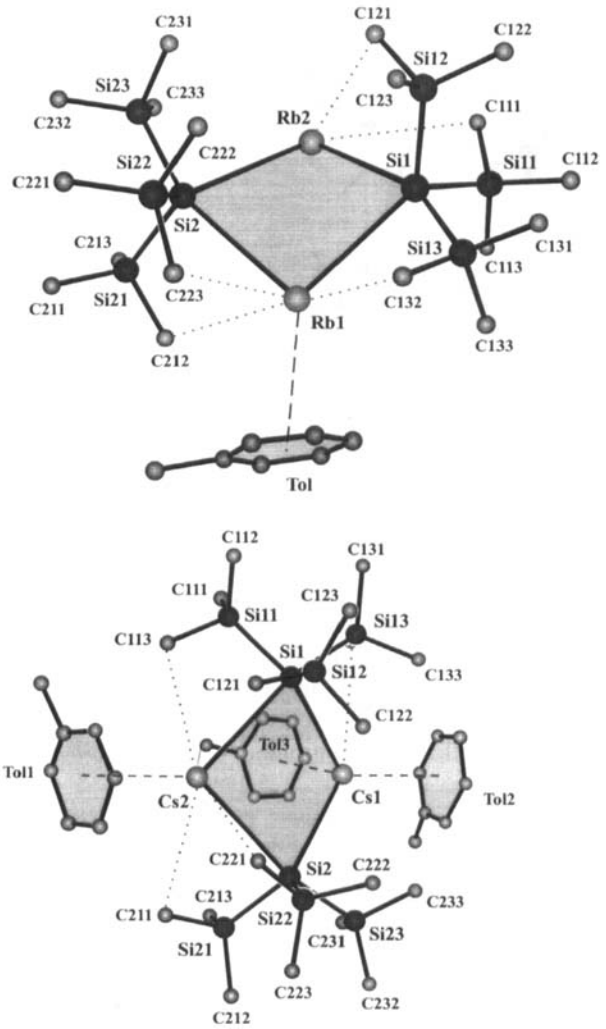

Figure 15. Top: Molecular structure of **3a**. Dotted lines indicate short intramolecular Rb···CH_3 contacts. Selected intramolecular distances [pm] and angles [°]: Rb1–Si1 361.6(4), Rb1–Si2 359.5(4), Rb2–Si1 352.2(4), Rb2–Si2 353.2(4), Rb···Rb 430.5(2), Rb1–C(tol1) 342(3)–391(3), Si1-Rb1-Si2 95.4(1), Si1-Rb2-Si2 98.3(1), Rb1-Si1-Rb2 74.2(1), Rb1-Si2-Rb2 74.3(1). Bottom: Molecular structures of **4a**. Dotted lines indicate short intramolecular Cs···CH_3 contacts. Selected intramolecular distances [pm] and angles [°]: Cs1–Si1 380.7(2), Cs1–Si2 385.0(2), Cs2–Si1 377.7(2), Cs2–Si2 377.4(2), Cs···Cs 492.0(1), Cs1–C(tol1) 368(2)–408(2), Cs1–C(tol2) 351(2)–390(2), Cs2–C(tol3) 368.0(7)–386.5(10), Si1-Cs1-Si2 92.0(1), Si1-Cs2-Si2 93.6(1), Cs1-Si1-Cs2 80.9(1), Cs1-Si2-Cs2 80.4(1).

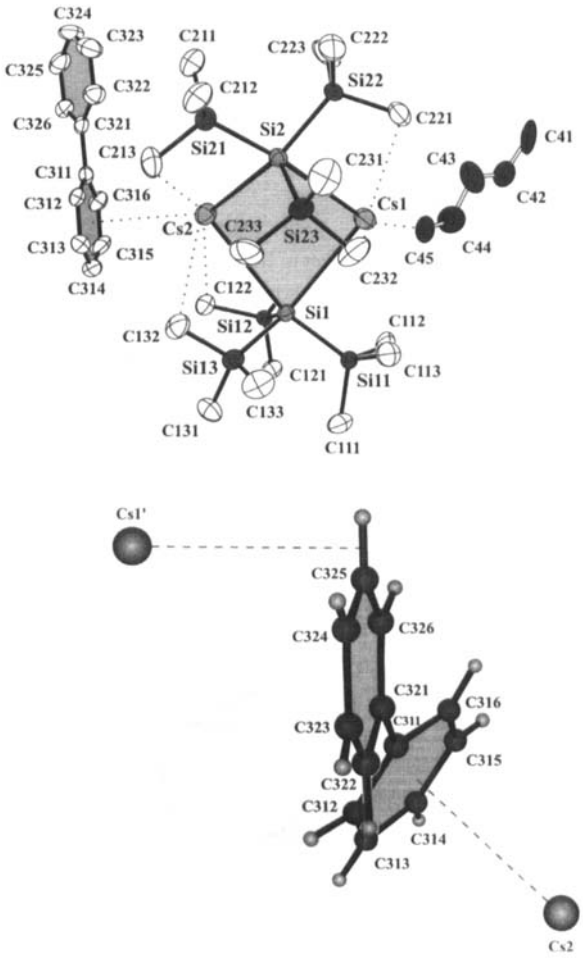

Figure 16. Top: Molecular structure of **4b** (ellipsoids at the 50% probability level). Dotted lines indicate short intramolecular Cs···CH_3 contacts. Selected intramolecular distances [pm] and angles [°]: Cs1–Si1 367.7(2), Cs1–Si2 374.2(2), Cs2–Si1 376.5(2), Cs2–Si2 381.1(2), Cs···Cs 463.7(1), Cs1–C325 368.3(7), Cs2–C311 383.6(5), Cs2–C312 375.3(5), Cs2–C313 373.3(6), Cs2–C314 380.9(6), Cs2–C315 385.9(6), Cs2–C316 386.6(6), Cs1–C41 (Cs1–C45) 385(1), Si1–Cs1-Si2 92.99(4), Si1-Cs2-Si2 90.52(3), Cs1-Si1-Cs2 77.06(3), Cs1-Si2-Cs2 75.74(3). Bottom: The biphenylene ligand acts as a η^6- and a η^1-ligand, thus bridging the Cs2 atom of one dimer and the Cs1′ atom of a second one.

methylsilyl groups; the latter lead to infinite zigzag chains of cesium hypersilanide dimers. Together with the above-mentioned linkage by biphenylene ligands, this produces a polymeric structure with layers parallel to (1 0 1) (Figure 17). Finally, the coordination sphere of Cs1 is completed by interactions with the terminal C–H bonds of a intercalated *n*-pentane, which is disordered within the layers over a crystallographic inversion center (Figure 17).

The solvate 4c: Addition of tetrahydrofuran, a strong σ donor, to a suspension of rubidium or cesium hypersilanide in pentane immediately produced orange-yellow solutions. On cooling to −60 °C, these only gave oily products containing approximately five to six equivalents of THF per hypersilanide moiety. Drying under high vacuum for 12 h at 40 °C and subsequent recrystallization from *n*-pentane yielded—in the case of the ce-

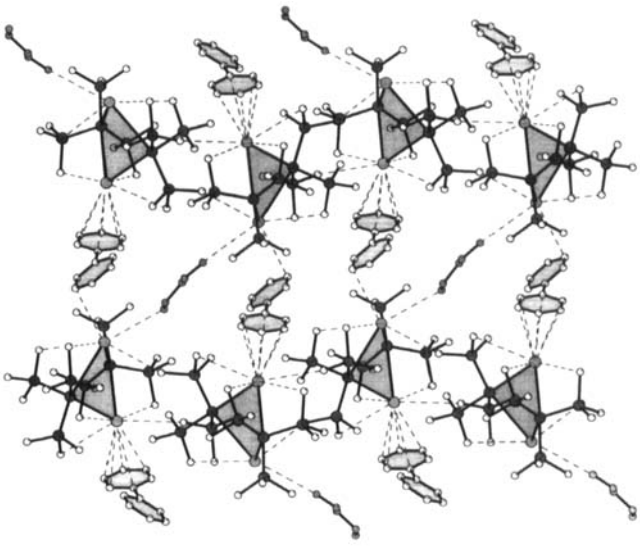

Figure 17. Formation of puckered layers of zigzag chains by linkage of the coordination polymers of **4b** through biphenylene and pentane molecules.

sium derivative—*colorless* crystals of **4c**, which, according to NMR spectra, still contain half an equivalent of THF per hypersilanide group.

$[CsSi(SiMe_3)_3]_2 \cdot THF$ **4c**

In the solid state, dimers with a virtually planar Cs_2Si_2 ring are present. Here the THF molecule acts as an intramolecular bridging ligand. The two cesium atoms are not coordinated by oxygen in the same manner (Figure 18, top). While the one short Cs2–O3 bond is nearly coplanar with respect to the best plane through the atoms of the THF molecule, the second longer Cs1–O3 bond is virtually perpendicular to this plane, so that two C–H bonds of both α-carbon are close to Cs1 and may act as additional electron donors (Figure 18, bottom). Intra- and intermolecular $Cs \cdots CH_3$ interactions complete the coordination spheres of the cesium atoms; the shorter intermolecular ones form double-layers, and the longer ones connect them further to produce a three-dimensional network (Figure 19).

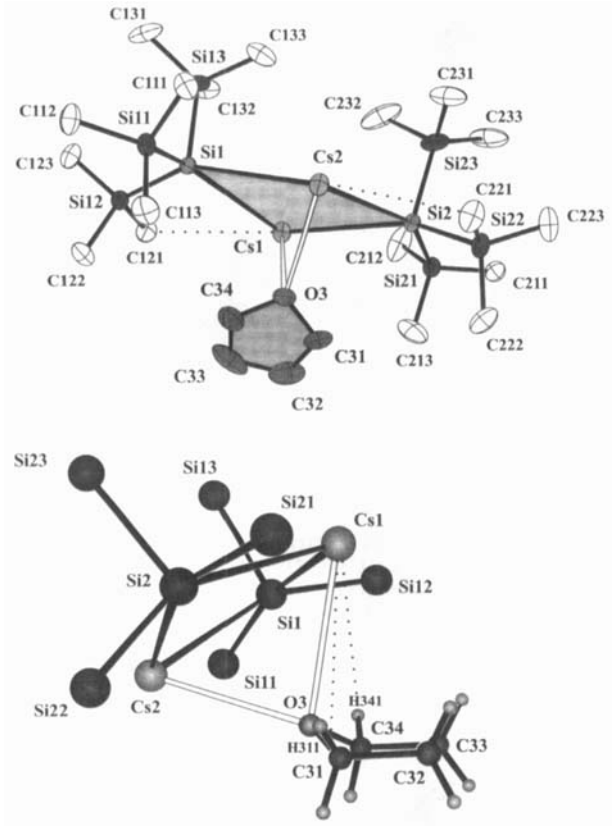

Figure 18. Top: Molecular structure of **4c** (ellipsoids at the 30% probability level). Dotted lines indicate short intramolecular $Cs \cdots CH_3$ and $Cs \cdots CH_2$ contacts. Selected intramolecular distances [pm] and angles [°]: Cs1–Si1 370.8(1), Cs1–Si2 367.3(1), Cs2–Si1 373.2(1), Cs2–Si2 369.9(1), Cs···Cs 419.63(5), Cs1–O3 328.1(3), Cs2–O3 309.7(3), Si1-Cs1-Si2 109.85(2), Si1-Cs2-Si2 108.73(2), Cs1-Si1-Cs2 69.02(2), Cs1-Si2-Cs2 69.04(2), Cs1-O3-Cs2 82.22(7). Bottom: Side-on coordination of the THF in **4c**. Cs1···C31 387.1(5), Cs1···C34 390.8(6).

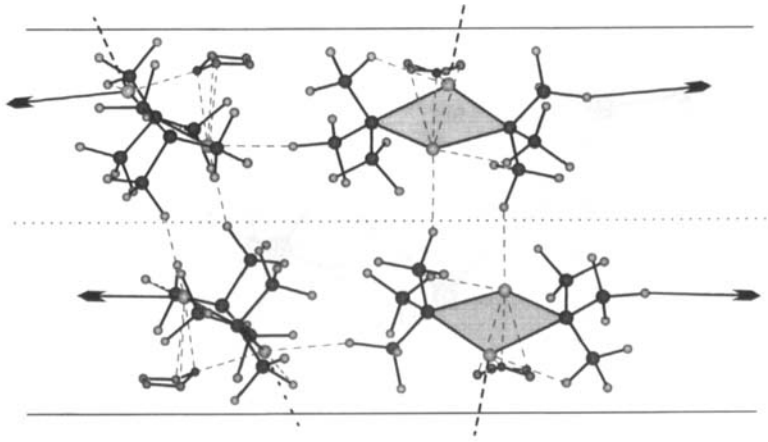

Figure 19. Double layers of dimers in **4c**. Dashed lines indicate short intra- and intermolecular $Cs \cdots CH_3$ and $Cs \cdots CH_2$ contacts. The arrows indicate further connections within the layers, whereas dashed lines signify short contacts between different layers.

Hypersilylated alkali metal stannanides: Alkali metal salts of a new, extremely bulky stannane were prepared (Scheme 3). Only a brief description of their syntheses is reported here, with a focus on the molecular structure of the sodium derivative. Further details of their chemistry and their physical properties will be discussed elsewhere.[18]

Recently, we were successful in preparing bis(hypersilyl)-stannylene (**6**) in high yields by treating alkali metal hypersilanides with $Sn[N(SiMe_3)_2]_2$ in *n*-pentane.[9b] Changing the reaction medium and the stoichiometry changed the products. In toluene/*n*-pentane and at temperatures below approximately −40 °C, mixtures of the stannylene **6** and an alkali metal stannanide bearing three hypersilyl ligands, $M^I-Sn[Si(SiMe_3)_3]_3$ were obtained (Scheme 3). Yields varied depending on the ratio of reactants, temperature, reaction time, and the alkali metal compound employed; a maximum of 61% was obtained for M = Na. At temperatures above −40 °C $M^I-Sn(CH_2Ph)[Si(SiMe_3)_3]_2$ were formed with release of toluene. The corresponding plumbanides, $M^I-Pb(CH_2Ph)[Si(SiMe_3)_3]_2$, were the only products obtained from analogous reactions with $Pb[N(SiMe_3)_2]_2$; no tris(hypersilyl)plumbanides have been detected so far. Sodium tris(hypersilyl)stannanide (**7**) was isolated as a pale yellow crystalline toluene solvate **7a** by recrystalliza-

$NaSn[Si(SiMe_3)_3]_3 \cdot toluene \cdot pentane$ **7a**

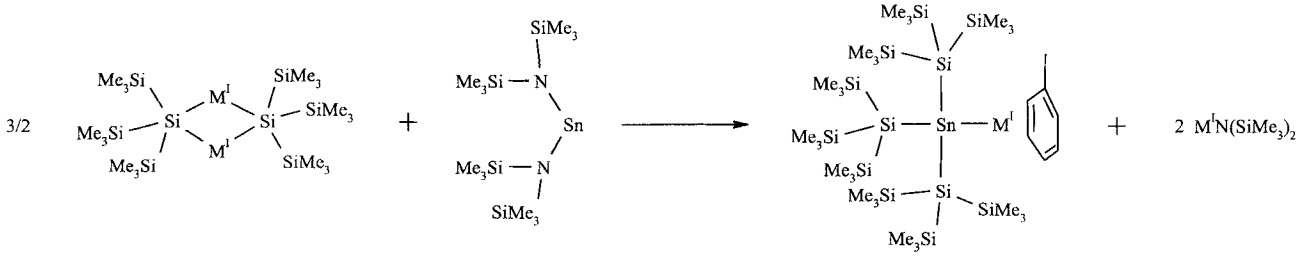

Scheme 3. Preparation of hypersilylated alkali metal stannanides × (M^I = Li, Na, K, Rb, Cs).

0947-6539/97/0309-1428 $ 17.50+.50/0 *Chem. Eur. J.* **1997**, *3*, No. 9

tion from mixtures of *n*-pentane and toluene. Although the crystals of **7a** are typically very small and tend to grow together in bunches, its crystal structure was determined on a small, but well-grown specimen.

Molecular structure of 7a: In contrast to most of the hypersilanides of the heavy alkali metals, this stannanide with its extremely bulky substituents is a monomer even in the solid state (Figure 20). The sodium cation is coordinated by the negatively charged tin atom and a (slightly disordered) η^6-coordinated

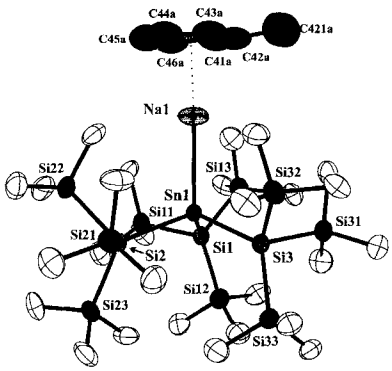

Figure 20. Molecular structure of **7a** (ellipsoids at the 30% probability level). Only one orientation of the disordered toluene is shown. Selected intramolecular distances [pm] and angles [°]: Na1 Sn1 307.0(5), Na1–C41a 290(4), Na1–C42a 282(5), Na1–C43a 289(4), Na1–C44a 290(4), Na1–C45a 294(4), Na1 C46a 292(4), Sn1–Si1 270.7(3), Sn1–Si2 270.2(3), Sn1–Si3 270.4(3), Na1-Sn1-Si1 109.6(1), Na1-Sn1-Si2 108.8(2), Na1-Sn1-Si3 108.7(2), Si1-Sn1-Si2 110.14(9)(4), Si1-Sn1-Si3 110.49(9), Si2-Sn1-Sn3 109.2(1).

toluene molecule. The observed Na–Sn distance of 307 pm is 16 pm shorter than the sum of the covalent radii, if the value for sodium from X-ray crystallography is used (Sn: 140 pm; Na 183 pm[14]). The Na–C distances to the ring atoms of the toluene molecule lie in the range 282–311 pm; their mean value of 291 pm is much shorter than that in the only sodium–toluene complex known to date, namely, the silylated alanate Na[Al(SiMe$_3$)$_4$]·(toluene)$_2$. In this alanate the sodium ion is tetrahedrally coordinated by two methyl groups of the alanate anion (Na···C 269 pm) and two η^6-aromatic rings (308 pm). Neither close intermolecular contacts to methyl groups, as found in the structures of **1a** and **1b**, nor any unusual interactions with the *n*-pentane molecules incorporated into the crystal lattice are observed for the stannanide **7a**.

While acute angles are theoretically predicted for stannanide anions and, indeed, are found in the two other structurally characterized alkali metal stannanides, (PMDTA)Li–SnPh$_3$[19a] and (toluene)$_3$K–Sn(*neo*-C$_5$H$_{11}$)$_3$,[19b] they are not observed for the tris(hypersilyl)stannanide anion in **7a**. Instead, the sterical requirements of the substituents leads to "normal" Si-Sn-Si angles of about 110° and to elongated Sn–Si bonds. These are 3 pm longer than in bis(hypersilyl)stannylene **6** and even 12 pm longer than in (Me$_3$Si)$_3$Sn–Sn(SiMe$_3$)$_3$.[20] As a further consequence of this steric stress, remarkable deformations within the hypersilyl substituents occur. The mean Si–Si bond length was determined to be 237 pm in **7a**, this is 3 pm longer than in the investigated alkali metal hypersilanides. The Sn-Si-Si angles are widened up to 126°, the Si-Si-Si angles are compressed down to 96.6°.

Conclusion

The hypersilanides of the alkali metals are readily synthesized and are valuable reagents for the synthesis of hypersilyl derivatives of other elements. All solvent-free derivatives are readily soluble in aromatic hydrocarbons, such as benzene or toluene, without deprotonation or reduction of the solvent under ambient conditions. However, their reactivity towards substrates, such as metal halides, amides, and alcoholates, remains high. In spite of the ionic nature of the bonding between the alkali metal and the hypersilyl substituent, the lighter hypersilanides (M = Li–K) are soluble in even aliphatic hydrocarbons. The main reason for this behavior is the formation of dimers, consisting of four ions with only small net dipole moments, which are covered by a lipophilic skin of trimethylsilyl groups. Nevertheless, interactions other than of the van der Waals type occur between these dimers. The C–H bonds of the trimethylsilyl groups act as electron donors, forming nearly linear Si–CH$_3$···M bridges, which are additionally strengthened by dipole–ion forces between the polar Si–C bond and the metal cations. Similar bridges are observed within the dimers, perhaps causing the inertness of the hypersilanides towards many organic solvents under ambient conditions. The peculiarities of the molecular and crystal structures, as well as the decreasing solubility from the lithium to the cesium derivatives, can also be traced back to these secondary forces. The bigger the metal ion, the greater the number of such Si–CH$_3$···M bridges formed. Solvent molecules that can act as σ or π donors, such as benzene, toluene, or THF, break down the network of Si–CH$_3$···M bridges, replacing them—at least partially—by stronger donor–metal interactions. In some cases even the ionic forces *within* the dimer are overcome, and monomers are formed, such as the benzene solvate **2b** or LiSi(SiMe$_3$)$_3$·(THF)$_3$.[21]

The tris(hypersilyl)stannyl substituent [(Me$_3$Si)$_3$Si]$_3$Sn- is even bulkier than the already very demanding hypersilyl group. It is accessible by the reaction of alkali hypersilanides with stannylene **6** under certain conditions. The monotoluene solvate of its sodium derivative, **7a**, is a monomer, even in the solid state, and contains a virtually linearly coordinated sodium ion. The overcrowding within this substituent leads to notable distortions of bond lengths and angles. Whether this substituent is capable of stabilizing unusual low coordination numbers for elements other than the alkali metals is currently under investigation.

Experimental Section

General: All reactions and manipulations were carried out under an inert atmosphere of argon by means of standard Schlenk techniques, unless otherwise stated. *n*-Pentane and *n*-heptane were distilled from LiAlH$_4$; benzene, toluene and THF from sodium benzophenone ketyl. Bis(hypersilyl)zinc was prepared by a reported procedure;[22] the alkali metals were purchased from commercial sources without further purification.

Raman spectra were recorded on a Dilor XY equipped with an argon laser (514.53 nm) on crystalline samples in sealed melting point tubes. NMR spectra were recorded on a Bruker AC250 (^{1}H, 250.133 MHz; ^{13}C, 62.896 MHz) or a Bruker AM200 (^{1}H, 200.133 MHz; ^{13}C, 50.323 MHz; ^{29}Si, 39.761 MHz) in [D$_6$]benzene, which had been degassed, distilled over Na/K alloy, and stored over a molecular sieve prior to use. C and H were determined by combustion with V_2O_5 as an additive and the alkali metals by titration with NaOH after ion exchange with H^+

  0947-6539/97/0309-1429 $ 17.50+.50/0

Preparation of $[NaSi(SiMe_3)_3]_2$ (1a) and $[KSi(SiMe_3)_3]_2$ (2a): A Schlenk flask was charged with $Zn[Si(SiMe_3)_3]_2$ (8.0 g, 14.27 mmol), a threefold excess of solid Na or K, a few pieces of broken glass pipettes, and a glass-coated magnetic stirrer. *n*-Heptane (50 mL (Na) or 100 mL (K)) was added, and the reaction mixture was refluxed under intense stirring for 12 to 16 h. The clear solution changed to a deep black suspension. The hot mixture was filtered through a prewarmed G4 glass filter. In the case of **2a**, the residue was washed with hot heptane (2×10 mL). The solution was then cooled and kept at $-20\,^{\circ}C$ for 1 d. Colorless crystals of **1a** or **2a** were obtained (**1a**: 6.33 g, 11.69 mmol, 82%; **2a**: 7.45 g, 12.99 mmol, 91%). A further 4% of **1a** was obtained by evaporation of the residual mother liquor to dryness, the oily residue treated with *n*-pentane (10 mL), and the resulting solution cooled to $-60\,^{\circ}C$ for 2 d. The compounds were characterized by C,H analysis, NMR (Table 1), and Raman spectroscopy (Table 2). As already observed for powders of **2a**,[1a] the crystalline compounds did not melt but decomposed, with a change of color to orange-brown, at about 130 °C; **1a**: calcd. C 39.94, H 10.06, Na 8.49; found C 39.61, H 10.12, Na 8.61; **2a**: calcd. C 37.69, H 9.49, K 13.63; found C 37.30, H 9.54, K 13.47.

General procedure for the synthesis of the solvated hypersilanides: A Schlenk tube was charged with the appropriate solvent-free alkali metal hypersilanide (2 mmol) and *n*-pentane (10 mL). The donor compound (benzene, toluene, biphenylene, THF) was added to the stirred mixture until the solution was clear. The mixture was then cooled to -30 to $-60\,^{\circ}C$. Most of the investigated solvates crystallized in virtually quantitative yields.

The resulting crystalline materials were characterized by ^1H and ^{29}Si NMR spectroscopy and elementary analysis. None of the compounds melted, but decomposed with a change of color (**4c**: ca. 130 °C) and release of solvent (**1b**, **2b**, **4b**). Since the NMR shifts of the solvates recorded in $[D_6]$benzene do not differ significantly from those of the solvent-free compounds or from the pure solvents, and their intensities are found in a ratio according to the crystallographic results, they are not listed here.

The C,H analyses gave only acceptable results for **4c**. The other solvates, **1b**, **2b**, and **4b**, probably lost solvent during the preparation procedure, since the determined proportion of carbon was much too low. **1b**: calcd. C 46.53, H 9.76, Na 7.42; found C 42.63, H 9.92, Na 7.93; **2b**: calcd. C 62.23, H 8.70, K 7.50; found C 57.32, H 9.04, K 8.34; **4b**: calcd. C 41.03, H 7.42, K 27.94; found C 40.20, H 7.15, Cs 29.13; **4c**: calcd. C 31.71, H 7.50, Cs 31.90; found C 31.59, H 7.54, Cs 32.08.

$NaSn[Si(SiMe_3)_3]_3 \cdot$ toluene $\cdot$ pentane (7a): A Schlenk flask was charged with $NaSi(SiMe_3)_3$ (2.00 g, 7.39 mmol), *n*-pentane (25 mL), and toluene (2 mL). After cooling to $-60\,^{\circ}C$, a solution of $Sn[N(SiMe_3)_2]_2$ (1.08 g, 2.46 mmol) in *n*-pentane was added dropwise under intense stirring. The solution immediately turned green-brown. It was held at this temperature for 24 h and then slowly warmed to room temperature. After filtering through a glass filter, it was again cooled to $-60\,^{\circ}C$, and the precipitated pale yellow crystals were recrystallized several times from a pentane/toluene mixture (10/1) to remove the simultaneously formed $NaN(SiMe_3)_2$. Yield: 1.57 g (1.50 mmol, 60.8%); decomp.: ca. 125 °C.; ^1H NMR (resonances of the Me_3Si groups only): $\delta = 0.47$ (s); ^{13}C NMR: $\delta = 7.2$; Anal. calcd C 44.65, H 9.32, Na 2.32; found C 41.42, H 9.24, Na 2.03, again the C,H analysis did not give acceptable results because of loss of the solvent.

Crystal structure analyses for 1a, 1b, 2a, 2b, 4b, 4c, and 7a: Crystals were poured into cool (10 °C), degassed Nujol and transferred into capillaries, which were sealed and immediately placed in the cold gas stream of a Siemens P3 or P4 four-circle diffractometer equipped with a low-temperature device. Unit cell dimensions were derived from the least square fit of the angular settings of 25–58 reflections. Data was collected in Wyckoff (P3) or adaptive omega scan mode (P4). Selected data collection parameters and other crystallographic data are summarized in Table 6. All structures were solved in the space groups derived from E-values and systematic absences using the direct methods implemented in the SHELXS-86 program.[24a] Because of twinning, special treatment was necessary for **2b** (see below).

The refinement based on F_o^2 values was performed by the full-matrix least-square method employing the SHELXL-93 program.[24b] Anisotropic displacement parameters were refined for the non-hydrogen atoms. The hydrogen atoms were treated isotropically. Their sites were refined freely with the

Table 6. Summary of the crystallographic data.

	1a	**1b**	**2a**	**2b**	**4b**	**4c**	**7a**
formula	$C_{18}H_{54}Na_2Si_8$	$C_{24}H_{60}Na_2Si_8$	$C_{18}H_{54}K_2Si_8$	$C_{27}H_{45}KSi_4$	$C_{32.50}H_{70}Cs_2Si_8$	$C_{22}H_{62}OCs_2Si_8$	$C_{39}H_{101}NaSi_{12}Sn$
M_r	541.32	619.42	573.53	521.09	951.42	833.25	1048.96
color	colorless	colorless	colorless	yellow	pale yellow	colorless	pale yellow
crystal size	$0.6 \times 0.3 \times 0.4$	$0.6 \times 0.4 \times 0.4$	$0.6 \times 0.6 \times 0.2$	$0.7 \times 0.6 \times 0.6$	$0.5 \times 0.3 \times 0.3$	$0.6 \times 0.3 \times 0.3$	$0.4 \times 0.1 \times 0.1$
crystal shape	prism	prism	rhombic platelett	prism	platelet	rhombic platelet	needle
system	triclinic	monoclinic	monoclinic	trigonal	monoclinic	monoclinic	orthorhombic
space group (no.)	$P\bar{1}$ (2)	$P2_1/c$ (14)	$P2_1/c$ (14)	$P3$ (143)	$P2_1/n$ (14)	$P2_1/c$ (14)	$P2_12_12$ (18)
a (Å)	12.490(1)	14.3343(11)	14.552(2)	15.7647(8)	15.327(4)	16.647(2)	21.849(7)
b (Å)	13.105(1)	23.466(2)	13.945(2)	15.7647(8)	15.395(4)	18.758(2)	21.368(7)
c (Å)	23.232(3)	12.540(2)	18.115(3)	11.6437(8)	20.649(6)	14.227(2)	13.533(4)
α (°)	92.733(9)	90	90	90	90	90	90
β (°)	103.264(10)	106.971(7)	91.02(1)	90	94.41(1)	107.56(1)	90
γ (°)	101.997(7)	90	90	120	90	90	90
V (Å^3)	3602.2(6)	4034.5(7)	3675.5(10)	2506.1(2)	4858(2)	4235.6(9)	6318(3)
Z	4	4	4	3	4	4	4
$F(000)$	2298	1352	1248	846	1948	1696	2256
ρ_{calcd} (g cm^{-1})	0.998	1.020	1.036	1.036	1.301	1.307	1.103
μ (mm^{-1})	0.328	0.300	0.525	0.315	1.717	1.961	0.662
instrument	P4	P4	P3	P4	P3	P3	P3
2θ range (°)	$3.2 < 2\theta < 45$	$3.4 < 2\theta < 52$	$4.5 < 2\theta < 52$	$3.5 < 2\theta < 52$	$3.2 < 2\theta < 48$	$3.3 < 2\theta < 52$	$3.3 < 2\theta < 48$
data measured	9806	8298	6731	4438	7855	8928	5419
unique data	9291 [$R_{int} = 0.037$]	7921 [$R_{int} = 0.055$]	6731	3806 [$R_{int} = 0.0479$]	7542 [$R_{int} = 0.0364$]	8928	5418 [$R_{int} = 0.1199$]
refl. used (N_o)	9259	7921	6731	3804	7542	8864	5175
parameters (N_p)	833	547	488	427	600	452	583
N_o/N_p	11.1	14.5	13.8	8.9	12.6	19.6	8.9
hydrogens	sites free; U's groupwise	free	free	sites free; U's groupwise	sites free; U's fixed	sites free; U's groupwise	riding
$wR2$ (all data) [a]	0.099	0.0928	0.1265	0.0842	0.115	0.112	0.163
weights a; b	0.0435; 0	0.0337; 0	0.0917; 0	0; 0	0.0338; 5.983	0.0509; 6.411	0.0314; 26.5
$R1$ ($F_o > 4\sigma(F_o)$) [b]	0.042	0.041	0.0484	0.034	0.040	0.041	0.060
GOF [c]	0.894	0.831	0.990	0.638	1.029	1.059	1.101
resid. density (e Å^{-3})	0.491/−0.280	0.585/−0.610	0.602/−0.582	0.162/−0.165	0.777/−0.774	1.188/−0.828	0.459/−0.516

[a] $wR2 = \{\sum[w(F_o^2 - F_c^2)^2]/\sum[w(F_o^2)^2]\}^{1/2}$ with $w^{-1} = \sigma^2(F_o^2) + (aP)^2 + bP$ ($P = \max(F_o^2, 0) + 2F_c^2)/3$. [b] $R1 = \sum(||F_o| - |F_c||)/\sum|F_o|$. [c] GOF $= \{\sum[w(F_o^2 - F_c^2)^2]/(N_o - N_p)\}^{1/2}$.

0947-6539/97/0309-1430 $ 17.50+.50/0 *Chem. Eur. J.* **1997**, *3*, No. 9

exception of those for which the atomic coordinates shifted to nonsense values; these were refined with common C–H lengths and H-C-H angles, riding on the appropriate carbon atom. Further details of the refinement and all remaining crystallographic data (excluding structure factors) for the structures reported in this paper have been deposited with the Cambridge Crystallographic Data Centre as supplementary publication no. CCDC-100267. Copies of the data can be obtained free of charge on application to The Director, CCDC, 12 Union Road, Cambridge CB21EZ, UK (Fax: Int. code +(1223)336-033; e-mail: teched@chem-crys.cam.ac.uk).

Crystal structure analysis of 2b: The crystal of **2b** was merohedrical twinned about a mirror plane (−1 −1 0) parallel to the crystallographic threefold axis. The method of Pratt, Coyle, and Ibers, as implemented in the SHELXL-93 program,[24b] was used to refine the fractional contribution of the twin domain (with corresponding index transformation being: $h' = -k$; $k' = -h$; $z' = z$) to give a value of 0.454(2).

Computational details for *the ab initio* calculations: The Gaussian 94 package[25] was employed for all calculations. The optimizations of the structural parameters of $MSiH_3$ and $M_2(SiH_3)_2$ molecules were performed using the 4-electron pseudo-potential for silicon and 9-electron pseudo-potentials for potassium, rubidium, and cesium of the Stuttgart group,[26] whereas for lithium and sodium all electrons were included in the calculations. The basis sets optimized for the pseudopotentials were partially decontracted (Si) and augmented by diffuse (Si) and polarization functions (Si, Rb, Cs).

Si: (4s4p1d)/[5s5p1d]: exponents: s: 4.014378, 1.393707, 0.251658, 0.100180, 0.03989; p: 1.102481, 0.583127, 0.208675, 0.069147, 0.022913; d: 0.28;

K: (5s4p1d)/[7s5p1d]: exponents: s: 8.223362, 3.797211, 1.331607, 0.666282, 0.272807, 0.037092; p: 21.605670, 1.100212, 0.504345, 0.317869, 0.148125, 0.022139; d: 0.794;

Rb: (5s4p1d)/[7s5p1d]: exponents: s: 4.727461, 2.930825, 0.601849, 0.466244, 0.246463, 0.053379, 0.021018; p: 5.608470, 3.452727, 0.754374, 0.327974, 0.141797, 0.020506; d: 0.55;

Cs: (5s4p1d)/[7s5p1d]: exponents: s: 5.800659, 4.298432, 1.807221, 0.388922, 0.175652, 0.031063, 0.013152; p: 3.738376, 2.110247, 0.558883, 0.281825, 0.119991; 0.015750; d: 0.40.

For Li and Na 6-311 G*(+), and for H Dunning's double-zeta correlation-consistent basis sets were used (as implemented in Gaussian 94[25]). The molecular structures of both the monomers and dimers were optimized by full MP2 calculations in maximal symmetry: C_{3v} (monomers), C_{2h} (II, III, IX), C_{2v} (IV, V, VIII), and C_s (VI, VII). For the idealized dimer structure I the Rb···Si bond lengths were restricted to be equal and D_{3d} symmetry was superimposed on the $H_3Si\cdots SiH_3$ fragment. The optimized structures had all been proven to be true local minima (except isomer I) by frequency calculations, showing no negative eigenvalue of the force constant matrix (Hesse matrix).

The charge distributions were all calculated using MP2 density and natural localized molecular orbitals (NLMO). The calculations have been performed employing the NBO module[27] of Gaussian 94. For the hypersilanide anion, the supersilanide anion, as well as for lithium hypersilanide and the lithium trihydrosilanide (used for comparison), Dunning's double-zeta correlation-consistent basis sets were used for H, C, and Si, whereas for lithium a 6-311 G*(+) basis (as implemented in Gaussian 94[25]) was employed.

Acknowledgment: I am grateful to Prof. Dr. Gerd Becker for his support of this work.

Received: March 12, 1997 [F637]

[1] a) K. W. Klinkhammer, W. Schwarz, *Z. Anorg. Allg. Chem.* **1993**, *619*, 1777; b) K. W. Klinkhammer, G. Becker, W. Schwarz in *Organosilicon Chemistry II* (Eds.: N. Auner, J. Weis), VCH, Weinheim **1996**.

[2] *Hypersilane* and *supersilane* were proposed as trivial names for tris(trimethylsilyl)silane and tri-*tert*-butylsilane, respectively, by N. Wiberg during the Xth International Symposium on Organosilicon Chemistry in Poznan (Poland).

[3] Reviews: D. Wittenberg, H. Gilman, *Quart. Rev.* **1959**, *13*, 116; D. D. Davis, C. E. Gray, *Organomet. Chem. Rev. A* **1970**, *6*, 283; W. P. Neumann, K. Reuter, *J. Organomet.Chem. Library* **1977**, *7*, 229; M. Paver, C. A. Russell, D. S. Wright, *Angew. Chem.* **1995**, *107*, 1679; *Angew. Chem. Int. Ed. Engl.* **1995**, *34*, 1545.

[4] Examples in: a) E. N. Gladyshev, E. A. Feodorova, L. O. Yuntila, G. A. Razuvaev, N. S. Vyazankin, *J. Organomet. Chem.* **1975**, *96*, 169; b) A. M. Arif, A. H. Cowley, T. M. Elkins, R. A. Jones, *J. Chem. Soc. Chem. Commun.* **1986**, 1777; A. M. Arif, A. H. Cowley, T. M. Elkins, *J. Organomet. Chem.* **1987**, *325*, C11.

[5] R. E. Benkeser, R. J. Severson, *J. Am. Chem. Soc.* **1951**, *73*, 1424; H. Gilman, T. C. Wu, *ibid*, *73*, 4031; H. Gilman, T. C. Wu, *J. Org. Chem.* **1953**, *18*, 753; E. Wiberg, O. Stecher, H. J. Andrascheck, L. Kreuzbichler, E. Staude, *Angew. Chem.* **1963**, *75*, 516; *Angew. Chem. Int. Ed. Engl.* **1963**, *2*, 507; H. Sakurai, A. Okada, M. Kira, K. Yonezawa, *Tetrahedron Lett.* **1971**, 1511; H. Sakurai, M. Kira, H. Umino, *Chem. Lett.* **1977**, 1265.

[6] a) T. F. Schaaf, W. Butler, M. D. Glick, J. P. Oliver, *J. Am. Chem. Soc.* **1974**, *96*, 7593; W. H. Ilsley, T. F. Schaaf, M. D. Glick, J. P. Oliver, *ibid.* **1980**, *102*, 3769; b) A. Sekigushi, M. Nanjo, C. Kabuto, H. Sakurai, *Organometallics* **1995**, *14*, 2630; c) A. Sekigushi, M. Nanjo, C. Kabuto, H. Sakurai, *Angew. Chem.* **1997**, *109*, 74; *Angew. Chem. Int. Ed. Engl.* **1997**, *36*, 113.

[7] a) G. Thirase, E. Weiss, H. J. Hennig, H. Lechert, *Z. Anorg. Allg. Chem.* **1975**, *417*, 221; b) M. A. Ring, D. M. Ritter, *J. Phys. Chem.* **1961**, *65*, 182;.c) E. Weiss, G. Hencken, H. Kühr, *Chem. Ber.* **1970**, *103*, 2868; d) O. Mundt, G. Becker, H. M. Hartmann, W. Schwarz, *Z. Anorg. Allg. Chem.* **1989**, *572*, 75.

[8] Investigations of alkali metal supersilanides $M^1Si(tBu)_3$—especially the solvent-free lithium and sodium derivative and a few solvates with M^1 = Na, K—are the subject of the following paper in print: N. Wiberg, K. Amelunxen, H.-W. Lerner, H. Schuster, H. Nöth, I. Krossing, M. Schmidt-Amelunxen, T. Seifert, *J. Organomet. Chem.* (Private communication by N. Wiberg).

[9] a) S. Henkel, K. W. Klinkhammer, W. Schwarz; *Angew. Chem.* **1994**, *106*, 721; *Angew. Chem. Int. Ed. Engl.* **1994**, *33*, 681; b) K. W. Klinkhammer, W. Schwarz; *Angew. Chem.* **1995**, *107*, 1448; *Angew. Chem. Int. Ed. Engl.* **1995**, *34*, 1334.

[10] K. W. Klinkhammer, W. Schwarz in *Organosilicon Chemistry III* (Eds.: N. Auner, J. Weis), VCH, Weinheim, in press.

[11] P. v. R. Schleyer, T. Clark, *J. Chem. Soc. Chem. Com.* **1986**, 1371; see also: B. T. Luke, J. A. Pople, M.-B. Krogh-Jespersen, Y. Apeloig, J. Chandrasekhar, P. v. R. Schleyer, *J. Am. Chem. Soc.* **1986**, *108*, 260; A. S. Zyubin, T. S. Zyubina, O. P. Charkin, P. v. R. Schleyer, *Russ. J. Inorg. Chem.* **1990**, *35*, 1044.

[12] a) K. Amelunxen, N. Wiberg, personal communication; b) W. P. Freeman, T. D. Tilley, G. P. A. Yap, A. L. Rheingold, *Angew. Chem.* **1996**, *108*, 960; *Angew. Chem. Int. Ed. Engl.* **1996**, *35*, 882.

[13] a) $K\text{-}C(SiMe_3)_3$: C. Eaborn, P. B. Hitchcock, K. Izod, A. J. Jaggar, J. D. Smith, *Organometallics* **1994**, *13*, 753; b) $Rb\text{-}C(SiMe_3)_3$ and $(C_6H_6)_3Cs\text{-}C(SiMe_3)_3$: C. Eaborn, P. B. Hitchcock, K. Izod, J. D. Smith, *Angew. Chem.* **1995**, *107*, 756; *Angew. Chem. Int. Ed. Engl.* **1995**, *34*, 687.

[14] C. Schade, P. v. R. Schleyer, *Adv. Organomet. Chem.* **1987**, 169.

[15] a) S. Cradock, G. A. Gibbon, C. H. van Dyke, *Inorg. Chem.* **1976**, *6*, 1751; E. Amberger, R. Romer, A. Layer, *J. Organomet. Chem.* **1968**, *12*, 417; b) H. Pritzkow, T. Lobreyer, W. Sundermeyer, N. J. R. van Eikema Hommes, P. v. R. Schleyer, *Angew. Chem.* **1994**, *106*, 221; *Angew. Chem. Int. Ed. Engl.* **1994**, *33*, 216.

[16] M. Brookhart, M. L. H. Green, *J. Organomet. Chem.* **1983**, *250*, 395.

[17] Similar interactions are also present in all alkali metal methanides. But note that here the methyl groups bear a full negative charge [review in E. Weiss, Angew. Chem. **1993**, *105*, 1565; *Angew. Chem. Int. Ed. Engl.* **1993**, *32*, 1501].

[18] K. W. Klinkhammer, manuscript in preparation.

[19] a) D. Reed, D. Stalke, D. S. Wright, *Angew. Chem.*, **1991**, *103*, 1539; *Angew. Chem. Int. Ed. Engl.* **1991**, *30*, 1459; b) P. B. Hitchcock, M. F. Lappert, G. A. Lawless, B. Royo, *J. Chem. Soc. Chem. Commun.* **1993**, 554.

[20] K. W. Klinkhammer, unpublished. The compound $(Me_3Si)_3Sn\text{-}Sn(SiMe_3)_3$ was investigated earlier [P. Mallela, R. Geanangel, *Inorg. Chem.* **1993**, *32*, 5623]. The authors did not recognize that the crystals were twinned and therefore their values for bond lengths and angles were falsified.

[21] A. Heine, R. Herbst-Irmer, G. M. Sheldrick, D. Stalke, *Inorg. Chem.* **1993**, *32*, 2694.

[22] J. Arnold, T. D. Tilley, A. L. Rheingold, S. J. Geib, *Inorg. Chem.* **1987**, *26*, 2106.

[23] G. Becker, H. M. Hartmann, A. Münch, H. Riffel, *Z. Anorg. Allg. Chem.* **1985**, *530*, 29.

[24] a) G. M. Sheldrick, *SHELXS-86, Program for the Solution of Crystal Structures*, University of Göttingen, Germany, **1986**; b) G. M. Sheldrick, *SHELXL-93, Program for Crystal Structure Refinement*, University of Göttingen, Germany, **1993**.

[25] *Gaussian 94, Revision D. 4.*, M. J. Frisch, G. W. Trucks, H. B. Schlegel, P. M. W. Gill, B. G. Johnson, M. A. Robb, J. R. Cheeseman, T. Keith, G. A. Petersson, J. A. Montgomery, K. Raghavachari, M. A. Al-Laham, V. G. Zakrzewski, J. V. Ortiz, J. B. Foresman, C. Y. Peng, P. Y. Ayala, W. Chen, M. W. Wong, J. L. Andres, E. S. Replogle, R. Gompeerts, R. L. Martin, D. J. Fox, J. S. Binkley, D. J. Defrees, J. Baker, J. P. Stewart, M. Head-Gordon, C. Gonzalez, and J. A. Pople, Gaussian, Inc., Pittsburgh PA, **1995**.

[26] Si: W. Kuechle, M. Dolg, H. Stoll, H. Preuss, *J. Chem. Phys.* **1991**, *74*, 1245; K, Rb, Cs: T. Leininger, A. Nicklass, W. Küchle, H. Stoll, M. Dolg, A.Bergner, *Chem. Phys. Lett.* **1996**, *255*, 274.

[27] *NBO Version 3.1* by E. D. Glendening, A. E. Reed, J. E. Carpenter, F. Weinhold, as implemented in *Gaussian 94*.

[28] H. Bürger, W. Kilian, *J. Organomet. Chem.* **1969**, *18*, 299.

  0947-6539/97/0309-1431 $ 17.50+.50/0